Dissertação de Mestrado

Inatel
Instituto Nacional de Telecomunicações

On the performance of Cooperative Vehicular Visible Light Communication Networks in Curved and Rectilinear Roadway Scenarios

DIEGO JELDÚ CUBA ZÚÑIGA

DEZEMBRO / 2020

ON THE PERFORMANCE OF CO-OPERATIVE VEHICULAR VISIBLE LIGHT COMMUNICATION NET-WORKS IN CURVED AND RECTI-LINEAR ROADWAY SCENARIOS

DIEGO JELDÚ CUBA ZÚÑIGA

Dissertação apresentada ao Instituto Nacional de Telecomunicações, como parte dos requisitos para obtenção do Título de Mestre em Telecomunicações.

ORIENTADOR: Prof. Dr. Samuel Baraldi Mafra.

COORIENTADOR: Prof. Dr. Jorge Ricardo Mejía Salazar.

Santa Rita do Sapucaí
2020

Zúñiga, Diego Jeldú Cuba
Z68o
On the performance of CooperativeVehicular Visible LightCommunication Networks in Curvedand Rectilinear Roadway ScenarioS. – Santa Rita do Sapucaí, 2020.
71p.
Orientadores: Prof. Dr. Jorge Ricardo Mejía Salazar e Prof. Dr. Samuel Baraldi Mafra.
Dissertação de Mestrado em Telecomunicações – Instituto Nacional de Telecomunicações – INATEL.
Inclui bibliografia.
1. Visible light communication (VLC) 2. Vehicle to vehicle (V2V) 3. Vehicle-to-Infrastructure (V2I) 4. Bit Error Rate (BER) 5. Cooperative Communication 6. Mestrado em Telecomunicações. I. Salazar, Jorge Ricardo Mejía II. Mafra, Samuel Baraldi. III. Instituto Nacional de Telecomunicações – INATEL. IV. Título.
CDU 621.39

Ficha Catalográfica elaborada pelo Bibliotecário da Instituição
CRB6-2718 – Paulo Eduardo de Almeida

Inatel

Instituto Nacional de Telecomunicações

ATA Nº 200: DEFESA DA DISSERTAÇÃO DE MESTRADO EM TELECOMUNICAÇÕES – ÁREA DE CONCENTRAÇÃO: ENGENHARIA ELÉTRICA

Autor: Diego Jeldú Cuba Zúñiga

No dia 02 de dezembro de 2020, às 10h, remotamente via Plataforma Teams, realizou-se a defesa de dissertação de mestrado em Telecomunicações, cuja área de concentração é Engenharia Elétrica, do Engenheiro Diego Jeldú Cuba Zúñiga, intitulada "On the performance of Cooperative Vehicular Visible Light Communication Networks in Curved and Rectilinear Roadway Scenarios". A banca julgadora foi composta por: Prof. Dr. Samuel Baraldi Mafra do Inatel, presidente, Prof. Dr. Evelio Martín García Fernández da Universidade Federal do Paraná – UFPR e Prof. Dr. Felipe Augusto Pereira de Figueiredo – Inatel. Houve participação também remotamente, do co-orientador Prof. Dr. Jorge Ricardo Mejía Salazar, de professores, funcionários, alunos do Inatel e outras pessoas. O presidente deu início aos trabalhos, anunciando ser esta a centésima nonagésima sétima defesa de dissertação do Curso de Mestrado em Telecomunicações do Inatel. Solicitou ao mestrando proceder a sua defesa, o que foi feito no tempo regulamentar. Em seguida, os membros da banca examinadora fizeram perguntas, solicitaram esclarecimentos e teceram comentários sobre o trabalho desenvolvido. Terminada a fase de arguição e debates, os membros da banca iniciaram a sessão de julgamento para a deliberação quanto ao resultado da defesa:

(X) Aprovada sem restrições, mas condicionada às eventuais revisões indicadas pelos membros da banca examinadora

( ) Aprovada com restrições e condicionada às revisões indicadas pelos membros da banca examinadora

( ) Reprovada

O presidente anunciou o resultado final e eu Gisele Moreira dos Santos, secretária do Curso de Mestrado em Telecomunicações, lavrei a presente ata que, aprovada, foi assinada pelos membros da banca examinadora. Santa Rita do Sapucaí, 02 de dezembro de 2020.

Samuel Baraldi Mafra

Prof. Dr. Samuel Baraldi Mafra

Garcia

Prof. Dr. Evelio Martín García Fernández

Felipe Augusto P. de Figueiredo

Prof. Dr. Felipe Augusto Pereira de Figueiredo

“Self trust is the first secret of success”

Ralph Waldo Emerson

To my parents, ***José*** *and* ***Gladys****, for always having believed in me, for their dedication, for the many hours of work that translate into infinite love and that I will always have in my heart. You are wonderful doing everything for the professional development and happiness of your children, I love you.*

To my sister ***Zuledy****, for the motivation, concern, affection and incentive from my early school, university and higher stage, always helping me to analyze things better.*

To my love ***Luanna****, for having accompanied me during this stage, giving me all the support I needed, the care, the talks about the path towards the objectives and for always trusting in my potential.*

Acknowledgements

To **God**, for giving me life and the possibility of realizing my dreams, for allowing me to learn from my mistakes, for always letting me to meet good people in my way. Thank for choosing things in the right moment and for gave me a wonderful family, whom I love with all my heart.

To my advisor **Samuel Baraldi Mafra** for all the support, the hours dedicated and his professionalism. Thank you for believing and trusting in my potentials, now I see everything I have achieved and I feel glad with what I have accomplished.

To my co-advisor **Jorge Ricardo Mejía Salazar**, for his support during the research process, deep analysis, tenacity to work and positive attitude facing challenges.

To my friend **Nataly Roque Guadalupe**, for having helped me from the beginning in my stay in Brazil, for the hours of study together and essentially, for made me know more about Inatel, thus being a greater motivation to leave my country and to decide to do a master's degree at this institution.

To my others colleagues from the master's degree with whom we share many moments of study, especially **Elvira Salvador Diogo**, **Flavia Larisse Fernandes**, **Vitor Alexandre Campos Figueiredo**, **Braian Nathan de Oliveira Andrade** and **Mateus do Prado Capistrano**. In some way you showed and offered me your support for the progress of my activities and consequently to be able to continue with my research work.

To my friends from the doctoral program, **Mauro Alexandre Amaro da Cruz** and **Lucas dos Santos Costa**, for having shown their support, solved my doubts in academic terms and especially Lucas for his support with the Latex tools for the format of this academic work.

To **Gisele Moreira dos Santos**, for all the support throughout my studies at Inatel. For their generosity, kindness and excellent work, always providing solutions with a high work commitment.

To the **Inatel Foundation** for the opportunity to study here in Brazil, in a high-level institution from which I take the best of the international experiences that I have had to live.

Diego Jeldú Cuba Zúñiga

Summary

List of Figures

List of Tables

List of Abbreviations and Acronyms

3D	Three Dimensional
5G	Fifth Generation
AWGN	Additive White Gaussian Noise
BER	Bit Error Rate
BP	Broadcast Phase
CP	Cooperative Phase
DH	Dual Hop
FD	Full Duplex
FET	Field Effect Transistor
FOV	Field of View
Gbps	Gigabits per second
HD	Half Duplex
IoE	Internet of Everything
ITS	Intelligent Transportation System
J/K	Joule per Kelvin
LED	Light Emitting Diode
LOS	Line of Sight
MAC	Media Access Control
MIMO	Multiple Input Multiple Output
OOK	On-Off Keying
PD	Photo Detector
PDR	Packet Delivery Ratio
RF	Radio Frequency
RSSI	Received Signal Strength Indicator
SINR	Signal-to-Interference and Noise Ratio
SNR	Signal-to-Noise Ratio
THz	Terahertz
V2I	Vehicle to infrastructure
V2V	Vehicle to Vehicle
VLC	Visible Light Communication

List of Symbols

α	Horizontal Inclination angle
A_p	Area of incidence at receiver
A/W	Photodetector responsivity has units amperes/watt.
B	System Bandwidth
β	Horizontal Inclination angle
D	Destination vehicle
δ_l	Represents the case in which the interferer vehicle causes interference to the receiver l
d_{kl}	Represents the distance between the transmitter and the receiver
$dsdx_{kl}$	Vertical distance between the transmitter and receiver. So correspond to the differential distances between S and D along the x axis.
$dsdy_{kl}$	Horizontal distance between the transmitter and receiver. So correspond to the differential distances between S and D along the y axis.
$dsdy_{s,r_r}$	Represents the distance betwen source S and the receiver of relay R along the y axis
E_{det}	Irradiance that falls within the spectral range of the receiver
η	Fixed PD Capacitance/area
G	Open loop channel gain
Γ	FET Channel noise factor
γ	Vertical Inclination angle
$g(\psi_d)$	Gain of the PD
I	Interferer vehicle
I_n	Noise Bandwidth Factor
K_b	Boltzmann Constant
$(k\|h)$	Represent the center of the semicircular section
$(s\|r_t\|i)$	Subindice used to indicate whether the corresponding cars are working as source (s) as a relay in the transmitting (r_t) or as an interferer (i) mode
L	Denotes the internal radius of the semicircular roadway section
$(r_r\|d)$	Subindice used to indicate whether the corresponding cars are working as destination (d) or as a receiving (r_r) mode
m	Order-Index
N	Number of bits
n	Internal refractive index
$\hat{n}_d$	Unitary vector normal to the receiver (PD)
N_{kl}	Represents the Gaussian additive noise at the node l
$\hat{n}_s$	Unitary vector normal to the transmitter (LED)

P_{bg}	Background Noise Power
$\phi_{1/2}$	Half value angle of an LED
ψ_d	Incident angle
ϕ_s	Irradiance angle
P_k	LED Power
ψ_c	FOV of the receiver
q	Electronic Charge
Q(·)	Function which represents the probability of a normal (Gaussian) random variable having a value grater than x standard deviations
R	Relay (R) vehicle moving along the same lane of destination vehicle (D)
$\mathcal{R}$	Transmission Rate
S	Source vehicle
σ^2_{shot}	Shot Noise
T_A	Ambient Temperature
T_c	Filter Transmission Coefficient
$\sigma^2_{\text{thermal}}$	Thermal Noise
θ_d	Rotation angle measured with respect to the x-axis for the PD axis.
θ_s	Rotation angle measured with respect to the x-axis for the LED axis.
T	Time domain
u_k	Message sent by the corresponding transmitter
$\overline{u_{k,l}}$	Distance between k and l along the u-axis
σ^2	Noise variance
$\overline{v_{k,l}}$	Distance between k and l along the v-axis
$(v_k\|u_k)$	Coordinates of the transmitter (k) in $v$axis
$(v_l\|u_l)$	Coordinates of the receiver l in $u$axis
W	Radiant intensity of the emitting LED
W_{approx}	Analytical spectral irradiance
$X(t)$	Instantaneous Input Optical Power
$y_{r_t,d}$	The received signals at the destination
y_{s,r_r}	The received signals at the relay
ζ	Detector Responsivity

Resumo

Cuba-Zuniga, D.J. Sobre o desempenho de Redes Cooperativas de comunicação veicular usando Luz Visível em cenários de vias curvas e retilíneas [dissertação de mestrado]. Santa Rita do Sapucaí: Instituto Nacional de Telecomunicações; 2014.

Uma comunicação veículo-a-veículo (V2V) segura, eficiente, robusta e de baixo custo usando o protocolo VLC com altas taxas de transmissão é uma candidata para aliviar o tráfego intenso e reduzir acidentes em ambientes com alta densidade de veículos. Ao contrário dos protocolos de radiofrequência (RF), onde a estabilidade da comunicação não pode ser garantida em ambientes densos, o VLC surgiu como uma alternativa revolucionária. Suas aplicações incluem controle de tráfego rodoviário e prevenção de acidentes por meio da troca de mensagens entre uma combinação de infraestrutura e outros veículos na estrada. Neste trabalho foi estudada uma comunicação V2V-VLC entre dois carros se movendo ao longo de diferentes cenários rodoviários: **(i)** uma única faixa de rodagem retilínea de três faixas e **(ii)** uma única faixa de rodagem curva de três faixas. Foi realizada uma implementação de protocolos de comunicação cooperativa full-duplex (FD) para evitar a interrupção na ausência de um canal de linha de visão (LOS) e foi descoberto que o FD V2V-VLC cooperativo teve resultados promissores para evitar interrupções de comunicação quando os carros estavam viajando em estradas curvilíneas. Os resultados deste trabalho podem ser estendidos para o caso do cenário de comunicação veículo-infraestrutura (V2I), que também pode ser promissor em situações de tráfego de baixa densidade de carros. Por outro lado, foi analisada uma comunicação VLC cooperativa dual-hop que opera com os protocolos half-duplex HD e FD em um cenário sujeito à interferência de outro veículo. Em particular, consideramos quatro veículos: origem, destino, retransmissor e um possível interferente. O desempenho do sistema é avaliado considerando a taxa de erro de bit (BER) e outras métricas de desempenho. Os resultados mostram que a comunicação cooperativa é uma solução eficaz para cenários onde a transmissão direta entre origem e destino não pode ser realizada. Os resultados numéricos são comparados para situações com e sem interferência a fim de mostrar o impacto no esquema cooperativo VLC proposto.

***Palavras-Chave*:** Comunicação de luz visível (VLC); Veículo para veículo (V2V); Veículo para infraestrutura (V2I); Taxa de erro de bit (BER); Comunicação Cooperativa

Abstract

Cuba-Zuniga, D.J. On the performance of Cooperative Vehicular Visible Light Communication Networks in Curved and Rectilinear Roadway Scenarios [Thesis for Master in Science Degree]. Santa Rita do Sapucaí: Instituto Nacional de Telecomunicações; 2014.

A secure, efficient, robust, and low-cost vehicle-to-vehicle (V2V) communication using the VLC protocol with high transmission rates is a candidate for alleviating high traffic and reducing accidents in dense vehicle environments. Unlike radio frequency (RF) protocols, where communication stability cannot be guaranteed in dense environments, VLC has emerged as a revolutionary alternative. Its applications include road traffic control and accident prevention by exchanging messages between a mix of infrastructure and other vehicles on the road. In this work was studied a V2V-VLC communication between two cars moving along different roadway scenarios: **(i)** a single three-lane rectilinear carriageway and **(ii)** a single three-lane curved carriageway. An implementation of full-duplex (FD) cooperative communication protocol has been performed to avoid disruption in the absence of a line-of-sight (LOS) channel and it has been found that the cooperative FD V2V-VLC has promising results for avoiding communication disruptions when cars were traveling in curvilinear roadways. Results in this work can be extended to the case of vehicle-to-infrastructure (V2I) communication scenario, which can also be promising in situations with low-car-density traffic. On another hand, we analyzed a cooperative dual-hop VLC communication which operates with HD and FD protocols in a scenario subject to interference from another vehicle. In particular, we considered four vehicles: source, destination, relay and a possible interferer. The system performance is evaluated considering Bit Error Rate (BER) and other performance metrics. The results show that cooperative communication is an effective solution for scenarios where direct transmission between origin and destination can not be performed. The numerical results are compared for situations with and without interference in order to show the impact in the proposed VLC cooperative scheme.

***Keywords*:** Visible light communication (VLC); Vehicle to vehicle (V2V) ; Vehicle-to-Infrastructure (V2I); Bit Error Rate (BER); Cooperative Communication

Chapter 1

Introduction

1.1 Contextualization

Visible Light Communications (VLC) in its basic form, like any other communication system, consists of a light emitting diode (LED) as a transmitter, in free space optical communications channel, and an image sensor or photo-detector (PD) as a receiver [1]. LED intensity can be modulated easily and quickly, without any risk to human eyes, that has motivated its cost-effective application for dual purpose, data transmission as well illumination [2]. Due to their improved energy consumption, smaller size, long lifespan, and switching speed, LEDs are replacing the conventional incandescent and fluorescent bulbs for diverse applications as automotive headlamps,traffic signals, advertising, general lighting, and medical devices [3–6]. Additionally, because of its positioning capabilities, improved security, scalability and resistance against weather conditions, VLC is an ideal candidate for vehicular communication applications [7–11].

The visible light spectrum (400 THz- 800 THz) offers a 10^3 times wider and unlicensed (low-cost of implementation) bandwidth compared to the radio frequency (RF) communication [12–14]. Since VLC features an unlicensed and potentially much larger bandwidth, this makes possible very high data rate communication as long as the optical band does not overlap with existing radio frequency bands, causing electromagnetic interference [15]. These advantages made the visible light communication (VLC) technology emerged as a revolutionary wireless communication paradigm [16–18], with operation rates on the order of gigabits per second (Gbps) for short and medium distances [19]. These data rates can also be boosted through the implementation of multiple-input and multiple-output (MIMO) communication techniques [20–23], promising for future 5G technologies, and allows the implementation of hybrid VLC-RF heterogeneous networks with improved communication performances [23, 24].

1.2 Analysis of Related Works

In VLC there is an interesting possibility of integrating it with cooperative models [25], with the aim of improving communication between origin and destination through the use of one or more relay vehicles. This communication system could work in half duplex (HD) or full duplex (FD) modes. In the first case, communication occurs in two time slots, the relay only receives or transmits at each moment, while for FD the relay transmits simultaneously with the source. In [26], a MAC protocol based on FD communication with improved performance was proposed and compared to HD through the reduction of packet collisions. But the success rate of a V2V-VLC communication is influenced by many factors such as attenuation, interference, noise, and solar irradiance. All of these effects have been extensively investigated in the available literature [27–32]. Signal attenuation, for example, is modeled on the VLC channel, while sunlight and external light sources are considered as shot noise effects [33, 34].

For example, the presence of nearby interfering vehicles, has recently been shown to decrease the allowed separation between origin and destination in [15, 35]. The most recent studies on VLC applied to vehicle-to-vehicle (V2V) and vehicle-to-infrastructure (V2I) communication have been dedicated to considering the effects of road humidity [36, 37], measuring the signal strength quantified by the indicator of received signal strength (RSSI) and packet delivery rate (PDR) [28], as well as its low off-target propagation to prevent information theft and interception techniques [16]. In [38], a more in-depth analysis was performed taking into account the combined reflection of diffuse and specular light rather than using an ideal Lambertian mode. VLC is also sensitive to changes in the network, where cars can loss the LOS communication, and then, HD and FD cooperative communication protocols are suitable to maintain the source-destination communication [26, 35, 39]. Due to the directional line-of-sight (LOS), associated to the visible light, there is no self-interference for a VLC-FD, in contrast to RF communications [40]. Furthermore, experimental measurements in [27] indicate that the VLC can be used reliably for distances up to 45 m in real road driving scenarios that, despite having reduced communication distances ($\sim$ 150 m in theoretical analyses) in compared to RF ($\sim$ 500 m), VLC manages to reduce spectrum scarcity in RF systems [41]. About vehicle positioning such as a convoy or platoon group, in [42] a Visible Light Position and Vehicle Pose Estimation (VLC-VPE) was proposed that was based on a VLC receiver (QRX), which can simultaneously provide high-speed communication, highly accurate measurement and resolution in estimating vehicle posture with centimeter-level accuracy. Despite these advantages, there are two major limitations, stemming from LOS communication, that must be overcome before the V2V-VLC implementation becomes a reality. First, interference from nearby emitting vehicles, ambient light sources, and disruption of communication by obstacles along straight roads. Second, the interruption of communication due to an incorrect alignment between the emitter LED and the photo-diode (PD) receiver. Although there is a large body of literature that addresses the first issue [15, 27–30], misalignment between the LED and PD axes has only been partially addressed. An important indicator for the calculations obtained is the bit error rate (BER), which is a reference to know the average number of bits received in error divided by the total number of bits received, in this way the quality of the communication link can be evaluated. The BER was modeled for a cooperative V2V-VLC taking into account HD communication in [43], the analysis considered the position and posture of the vehicles. Although a hybrid VLC-RF approach can be implemented [44], it can be expensive and technically complex. Therefore, more research is needed on VLC to properly address this drawback. In particular, the prior literature is primarily limited to the effects of misalignment on communication performance for automobiles communicating between two different lanes along a straight highway [9, 11, 27, 39, 45].

1.3 Contributions

From the beginning of the research process about the VLC technology, it was captivating to know the different benefits that indicated its application. The possibility of transmitting data wirelessly, without worrying about regulating the use of spectrum, draws a lot of attention. In addition, the benefit of having a vast bandwidth and being able to establish more secure communications through its use, due to communications using VLC are directive. In fact, it does not leave a security breach because of the effect of intermediary interceptions outside the communication process as occurs in RF communication, where an intruder could try to get information which is spread in the environment, this not occurs in VLC communication thanks to its highly directivity an reduced FOV.

Regarding the application of VLC technology for vehicular networks, it was verified that there were no previous analyzes of full-duplex cooperative communications in scenarios of straight and curved roads, nor on that transition of the two types of roads during the communication process. In addition, an analysis of the effect of interference in the communication process has not been treated in detail in literature.

Among the contributions of this research work are, the bibliographical and conceptual review of the innovative technology for wireless communications using the spectrum of visible light VLC, which is presented in chapter 2. This review contains the operation, applications and an approach to its study in vehicular networks, where the architecture of the system is presented together with its key concepts.

In relation to the detailed above, the vehicular communication was analyzed evaluating two communication scenarios with real dimension measures and type of roadway in order to consider a more realistic scenario.

Finally, the last contribution of this work is the development of algorithms and the execution of simulations that allowed evaluating the scenarios and cases raised, thus giving the possibility of discussing the results and serving as an input for future works that may continue with this line of research.

1.4 Publications from this Work

The following articles were produced as a result of research related to this work:

❶ **Visible Light V2V Cooperative Communication Under Environmental Interference**. IXXXVII Brazilian Symposium of Telecommunications and Signal Processing, (SBrT). Petropolis, RJ, July 26th. 2019.

❷ **Cooperative Full-Duplex V2V-VLC in Rectilinear and Curved Roadway Scenarios**. Sensors 2020, 20, 3734. Basel, Switzerland, June 28th. 2020.

Chapter 2

Visible Light Communication

Visible light communication (VLC) is a wireless communication technology, which uses white or coloured LEDs to provide information through visible light spectrum [16]. LED is suitable as an optical signal-sending device, because of its light intensity can be modulated at high speed in comparison with traditional lighting devices such as incandescent bulbs and fluorescent lamps. Additionally, LEDs are already used for lighting and signage in many applications with high energy efficiency, a long lifespan and inexpensive cost [46]. VLC systems use visible light for communication, occupying the spectrum in the range of 380 nm to 750 nm, which corresponds to a frequency spectrum between 430 THz to 790 THz [29]. The huge spectrum available allows VLC to reach very high data rates that currently can reach a few tens of Gb/s [47], [48]. Furthermore, given that this data rate was achieved in less than a decade after the development of VLC systems began, it is obvious that the potential of the technology is even greater [12].

2.1 Applications

The easy availability, low cost, high data rates and broad spectrum of VLC can make it an important wireless communication technology as it would suit different types of future future applications. Here are some potential applications of VLC.

Intelligent Transport System

Intelligent Transport System (ITS) systems aim to increase the safety and efficiency of the transportation system, traffic flow as well as to reduce the environmental pollution by connecting vehicles, humans and roads through information and communications technologies [1] [49]. In [50], [38] , VLC is proposed for ITS communication to complement or replace the existing crowded RF-based communication. On the other hand, in [51] the authors considered VLC-based ITS systems to avoid accidents, specifically, when the fleet of locomotive trucks passes through intersections. VLC has been used to send acceleration, deceleration and braking signals to Road Site Unit (RSU) devices. For example, to reduce the amount of emergency braking or lane change in a complex environment, a fleet of trucks can send a VLC signal to the RSU, so can set a green signal or a fast route for other vehicles.

LiFi

Ligh-Fidelity (LiFi) technology consists of a wireless network system that includes a bi-directional multiuser communication. It involves multiple access points that forms the wireless network of small optical attocells with seamless handover [52]. LiFi is destined to replace or complement RF communication, for instance in places with overcrowded Wi-Fi networks. LiFi uses light-emitting diodes (LEDs) to transmit the data [53]. On the other hand, in areas that are sensitive to electromagnetic radiation (such as airplanes), Li-Fi technology may be a solution. Li-Fi also supports the Internet of Things (IoT). Speeds of up to 10 Gbits / s can be achieved that is 250 times faster than ultrafast broadband speed [29] [54].

Smart Cities and Smart Homes

Smart cities are expected to provide optimal connectivity between people, government, infrastructure, the economy, and the environment [55] [56]. Most of the functional entities of a 'smart city' are already available around us. However, reliable, sustainable, high-data-speed wireless connectivity is the 'bottleneck' to connecting everything as one. These applications can increase energy efficiency and human comfort by integrating multiple services in the lighting infrastructure. The most popular VLC application is indoor positioning, enabling navigation and augmented reality [57].

Hospitals

Due to VLC's nanometric wavelength, it cannot penetrate objects, this characteristic makes it ideal for applications where data confidentiality is very important. The inherent security and data protection feature of VLC provides a wireless communication alternative that could be used to lessen the health risks associated with radio frequency radiation. One such application area is hospitals, where VLC can be used to monitor patients, have machine-to-machine communication, patient record keeping, and all other networking applications. [58] [1]. Another benefit of its use in hospitals, is that it will not interfere with radio waves of the other machines,such as magnetic resonance imaging (MRI) scanners [59].

Underwater Communications

RF waves do not propagate optimally in seawater due to its good conductivity, therefore VLC communication should be used in underwater communication networks [60]. The Un Tethered Remotely Operated Vehicle (UTROV) is another underwater communication application using VLC. The different jobs that can be done with UTROV include the maintenance of the ocean observatory and the deployment of ships. In [61], among three QAM modulations, for a submarine communication system, a rate of 2.17Gb/s was obtained. In [60] was studied the impact of submarine communication channels using underwater visible light (UVLC), this study includes different communication link parameters. At [62], a bidirectional experimental transmission compatible with the 10Base-T standard was performed at a speed of 10 Mbit/s using a Manchester encoded signal.

2.2 VLC applied to Vehicular Networks

Although the VLC technology was initially intended for fast internet connection links in indoor environments, last decade has witnessed an increasing interest in its application for autonomous vehicles and intelligent transportation systems (ITSs), under an ever increasing number of vehicles per year, to provide safety and improved highway traffic flows [63–65]. In the context of vehicular communication, data is transferred from vehicle-to-vehicle (V2V) and from vehicle-to-infrastructure (V2I) [37]. They perform transmissions of security messages, which help to reduce, alert and prevent accidents by up to 81% [11]. This later application is of major importance for future safe autonomous vehicle networks [7, 51, 66].

2.2.1 System overview

A VLC system is composed by a VLC transmitter, which modulates the LED emmitted light, a VLC receiver based on photodetector like a photo-diode or an image sensor like a camera. The function of the receiver is to extract the modulated data signal from the light beam. Is important to know that both transmitter and receiver are apart each from other but linked by the VLC beam while they maintain the Line of Sight (LOS) [33].

Transmitter

The VLC emitter converts the information into messages that can be transmitted through the free space optical medium by using visible light with LEDs and lasers. An important component of the VLC transmitter is the encoder which converts the data into a modulated message [33].The encoder commands the switching of the LEDs according to the binary information and a specific data rate [67]. High bandwidth and high data rates are some of the advantages of using RGB LEDs for white light generation. Although, the disadvantage is the high complexity and modulation difficulties [29]. The data rate is subject to the switching of the LEDs, the propagated service is dependent on the transmit power and consequently the illumination pattern resides in the inclination of the angle of the transmitter [68], [69], [70].

Receiver

The classic VLC receiver consists of an amplification circuit, an optical concentrator, and an optical filter as illustrated in [71]. The bifurcation of the beam light when illuminating large areas is reduced, but the optical concentrator is used to compensate for this type of attenuation. In the VLC receiver, light is detected by a photodiode (PD) or camera and then converted to photocurrent, the former being preferable in the case of a stationary receiver; however, the image sensor is used instead of a PD due to the larger field of view in mobile situations. The way that interference is addressed is by implementing optical filters to mitigate the ’DC’ noise components present in the received signal [29].

Modulation techniques

Modulation is one of the main processes in the communication system. Proper and powerful modulation techniques allow for improved performance. In the case of VLC, its performance is likely to be affected by path loss and shot noise that are caused by natural and artificial light sources [72]. Modulation in VLC is achieved by applying variations in the intensity of the light sources that correspond to the information in the message [29].

On-Off Keying (OOK)

On-Off-Keying is the most simple form of amplitude-shift keying (ASK) modulation, it represents the digital data values by switching the status of the carrier wave. In its most simple form, carrier presence for a specific duration time is represented by a binary one, while its dimming and decrease of intensity for the same duration represents a binary zero [72].

Pulse Width Modulation (PWM)

Although On-Off Keying provides many advantages such ease of implementation and simplicity [73], its major drawback is the lower data rates, maninly at providing different dimming levels [41]. This has motivated the design of others modulation schemes based on pulse width and position. Pulse Width Modulation (PWM) is an efficient way to achieving modulation and dimming through the use PWM [74], [75], [29]. The widths of pulses are adjusted taking in consideration the desired level of dimming and the pulses carry the square wave modulated signal. The data rate of the modulated signal should be adjusted based on the dimming requirement [41].

Color Shift Keying (CSK)

Color Shift Keying (CSK) is a modulation type which was first proposed by the IEEE 802.15.7 standard for visible light communication [73]. A majority of VLC systems use a blue LED and a yellow phosphor layer on LEDs which converts the blue light into white but the downside is that the phosphor layer has a long relaxation time and it limits the maximum modulation frequency. By another hand, CSK exploits the design of RGB LED fixtures which use three separate LEDs to generate different colors. Among them white which is obtained using Red, Green and Blue mixture. CSK modulates the signal by changing the intensity of this three colors [76] [29] [41]. Unfortunately, the RGB LEDs are more expensive and need a complex control circuit to create white light, because of that RGB LEDs are less used in commercial devices at the moment [77].

2.2.2 Key Concepts

Line of Sight (LOS)

Since VLC requires direct LOS between sender and receiver, the narrow signal reception angle reduces mobility. However, for use in vehicular communications, VLC must also fully comply with vehicle mobility [33]. The directionality of the optical VLC transmission offers an advantage as only a small number of neighboring vehicles, within direct LOS of the receiver (Rx), are low in the same containment domain. The advantages are the significantly reducement of collision probability and the increasing scalability [78], also link scenarios that maintain LOS maximizes power efficiency and minimizes multipath distortion [79]. With respect to security, LOS requirement makes communication more secure, against potential attacks of interception [80], [28]. Visible light signals do not pass through all objects, they are only reflected off them, which is a coverage disadvantage and also a safety advantage [81], [82], [83].

Field of View (FOV)

The Field of View (FOV) is the angular range size the receiver is able to detect using its photo-diode (PD) detector. In [84], the FOV was expressed as the maximum angular size of the PD in a platoon scenario where the main challenge was to follow sharp trajectories. While FOV is smaller, it is less susceptible to interference from the environment [33]. For example, solar radiation is a type of noise that can degrade system performance and make it more unstable [85], [86].

Bit Error Rate (BER)

The Bit Error Rate (BER) is, in simple terms, the dimensionless average number of bits received in error, divided by the total number of bits received. BER can be measured before or after the error correction phase. These measurements are sometimes called pre-corrected BER and post-corrected BER. The pre-corrected BER is the best indication of channel performance, but the post-corrected BER is the best indication of the signal quality that the user will experience [87].

Signal to Noise Ratio (SNR)

Signal to Noise Ratio (SNR) is considered as VLC capability measure. SNR can be expressed as the ratio of the received visible light power and ambient noise [88]. The performance of a VLC communication is analyzed in terms of SNR, BER and data rate as has been studied in the literature [10, 38, 85, 89].

In the next chapter, the system model and bit error rate analysis of two scenarios will be studied, one straight roadway and a curved roadway. This system model also covers the interference impact in a network cooperative vehicle communication.

Chapter 3

Vehicular Visible Light Communications

In this chapter, an analysis of the vehicle-to-vehicle (V2V) visible light communication (VLC) between two cars moving along different roadway scenarios: (i) a multiple-lane rectilinear roadway and (ii) a multiple-lane curvilinear roadway is presented.

3.1 System Model

3.1.1 Straight Roadway Scenario

As schematically shown in Figure 3.1, the system consists of three cars; namely, the source (S), the destination (D) and an intermediary relay (R) vehicle, moving along a three-parallel-lane highway (running along the y-axis in Figure 3.1). The lanes are considered identical, having 3.5 m widths and centers at 1.75 m, 5.25 m and 8.75 m in relation to the x-axis in Figure 3.1.

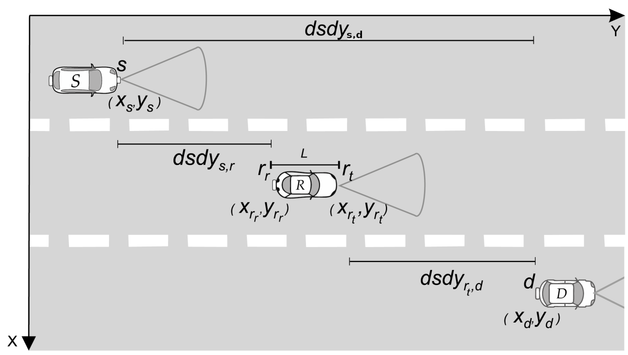

Figure 3.1: *Schematic of a V2V-VLC cooperative network with an intermediate relay vehicle.*

For the sake of generality, we consider a three-dimensional (3D) model for the VLC link (LED-PD) in Figure 3.2. $\hat{n}_s$ and $\hat{n}_d$ are used to represent the unitary vectors normal to the transmitter (LED) and receiver (PD) axes, respectively, which, in general, can be slightly tilted by α (γ_s) and β (γ_d) with respect to the y-axis (z-axis), as depicted. The irradiance (ϕ_s) and incident (ψ_d) angles were obtained from [39]

$$\phi_s = \arccos\left(\sin\gamma_s \cos\left[\alpha - \arctan\left(\frac{dsdx_{kl}}{dsdy_{kl}}\right)\right]\right), \tag{3.1}$$

$$\psi_d = \arccos\left(-\sin\gamma_d \cos\left[\beta - \arctan\left(\frac{dsdx_{kl}}{dsdy_{kl}}\right)\right]\right), \tag{3.2}$$

where $dsdy_{kl}$ and $dsdx_{kl}$ represent the horizontal and vertical distances between the transmitter and receiver, respectively. Subindices $k \in \{s, r_t\}$ and ($l \in \{r_r, d\}$) are used to indicate whether the corresponding cars are working as source (s), destination (d) or as a relay in the transmitting (r_t) or receiving (r_r) mode, respectively. Due to IR light

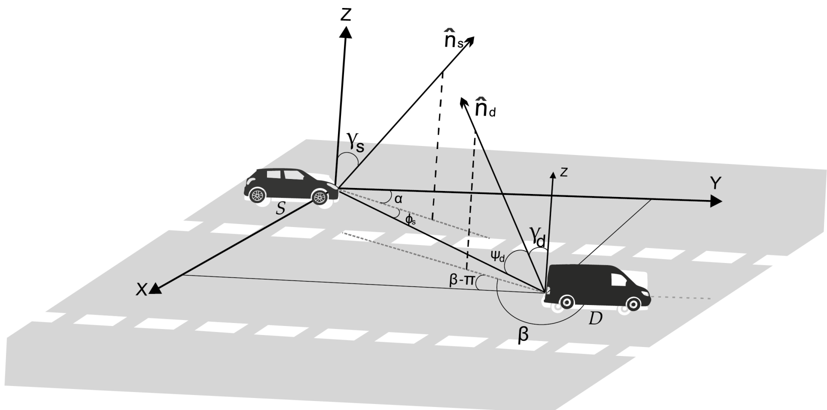

Figure 3.2: *3D graphical representation of two cars S and D using V2V-VLC along a three-lane roadway. γ_s and γ_d represent the vertical tilt angles of the LED and PD, respectively, whereas ϕ_s corresponds to the irradiance angle with respect to $\hat{n}_s$. α and β denote the horizontal tilt angles with respect to $\hat{n}_s$ and $\hat{n}_d$, respectively. ψ_d indicates the incidence angle with respect to $\hat{n}_d$. The unitary vectors $\hat{n}_s$ and $\hat{n}_d$ are used to denote the transmitter (LED) and receiver (PD) axes; i.e., they are normal to the corresponding surfaces.*

and visible light are close in wavelength and has qualitatively similar behavior, we can obtain the frequency response of a VLC channel starting from that the IR channels are relatively flat near DC [79]. The most important quantity at modeling a channel is the DC gain $H(0)$, which shows the transmitted and received average power. The average transmitted optical power P_t is described as below,

$$P_t = \lim_{T\to\infty} \frac{1}{2T} \int_{-T}^{T} X(t)dt, \tag{3.3}$$

where $X(t)$ represents the instantaneous input optical power and T the time domain.

The average received optical power is defined as follows,

$$P = P_t H(0), \tag{3.4}$$

where $H(0) = \int_{-\infty}^{\infty} h(t)dt$. In LOS links, being directed, hybrid, or non-directed situations, the DC gain $H(0)$ can be computed accurately by taking in consideration only the LOS propagation path. The following approximation is particularly accurate in LOS links,

$$H_{kl}(0) = \begin{cases} \frac{\mathrm{W} A_{\mathrm{p}} T_c}{d_{kl}^2} g(\psi_d) \cos(\psi_d) & , \quad 0 \leq \psi_d \leq \psi_c, \end{cases} \tag{3.5}$$

This last equation, will be used here to estimate the achievable signal-to-noise ratio (SNR) for a fixed transmit power. $d_{kl} = \sqrt{(dsdy_{kl})^2 + (dsdx_{kl})^2}$ represents the distance between the transmitter and the receiver; A_{p} is the area of PD; T_c is the filter transmission coefficient; and W and $g(\psi_d)$ are the radiant intensity of the emitting LED and the gain of PD, respectively. $\psi_c < \pi/2$ is used for the aperture angle of the concentrator, also named the PD field-of-view (FOV). Considering the LED as an ideal Lambertian surface, the radiant intensity can be described by the following equation.

$$\mathrm{W} = \left[\frac{(m+1)}{2\pi}\right] \cos^m(\phi_s), \tag{3.6}$$

with $m = -\ln 2/\ln\left[\cos\left(\phi_{1/2}\right)\right]$ indicating the order-index, where $\phi_{1/2}$ is the half-value angle of the LED. $g(\psi_d)$, on the other hand, depends on the FOV and the PD refractive index (n) as below

$$g(\psi_d) = \begin{cases} \frac{n^2}{\sin^2(\psi_c)} & , 0 \leq \psi_d \leq \psi_c, \\ 0 & , \psi_d \geq \psi_c. \end{cases} \tag{3.7}$$

all equations detailed above (3.3 - 3.7) were obtained from [79]

3.1.2 Curved Roadway Scenario

The idea in this section is to extend the previous modeling to the case of V2V-VLC in the presence of curved roads. In contrast to the previous section, where the LED and PD axes were fixed parallel to the y-axis, i.e., $\alpha = 0$ and $\beta = \pi$ (see Figure 3.2), we must now consider them to be rotating around the x-axis when traveling along a curved roadway. Rotation angles are measured with respect to the x-axis, as illustrated in Figure 3.3, and labeled as θ_s and θ_d for the LED and PD axes; i.e., $\alpha = \theta_s$ and $\beta = \pi - \theta_d$. $L = 20$ m is the radius of the internal border of the semicircular roadway, as depicted. The coordinate (k, h) $[(y, x)]$ is used to represent the center of the semicircular section, where $k = 29$ m and $h = 50$ m.

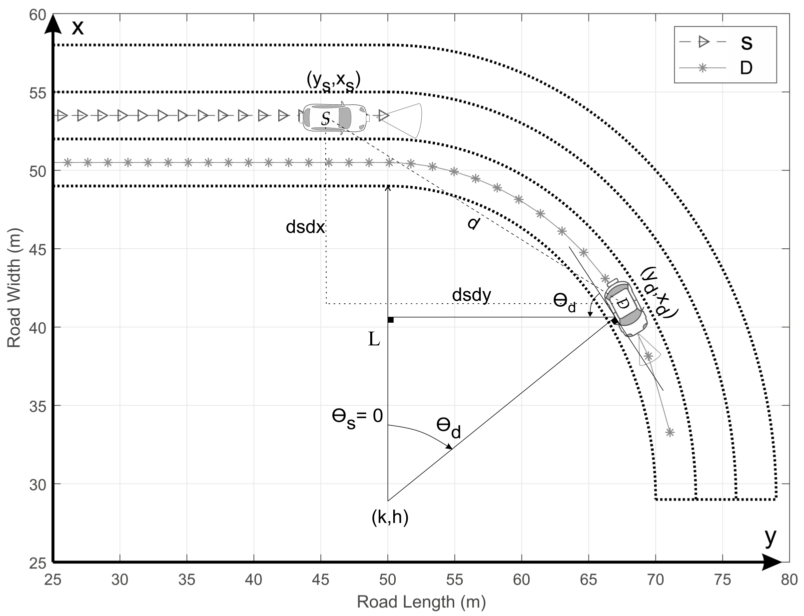

Figure 3.3: *Schematic of two cars using V2V-VLC along a curved roadway. θ_s and θ_d represent the rotation of the LED- and PD-axis with respect to the x-axis, respectively. L denotes the internal radius of the semicircular roadway section. $dsdx$ and $dsdy$ correspond to the differential distances between S and D along the x and y axes.*

For comparison purposes, we will consider both the cooperative and non-cooperative communication mechanisms. In the non-cooperative communication we used the scenario represented in Figure 3.3, whereas for the cooperative one we considered the scenario illustrated in Figure 3.4. In the cooperative scenario, we use the car R moving along the same lane of the car D, as depicted in Figure 3.4. For simplicity, all the calculations were made considering $\theta_s = 0$.

Our study of the V2V-VLC in this section is limited to the scenarios represented in Figures 3.3 and 3.4, i.e., for $y_s \leq h$. The corresponding vehicle lengths are considered as $l_s = l_d = 5$ m. The geometrical analysis of Figure 3.3 can be divided into two different situations. First, for $y_s \leq (h - dsdy_{sd})$, i.e., $y_d \leq h$, the V2V-VLC occurs along a rectilinear roadway ($\theta_s = \theta_d = 0$), analogously to the previous chapter. Second, for $(h - dsdy_{sd}) < y_s \leq h$, S continues traveling along a rectilinear path ($\theta_S = 0$), whereas D enters into the semicircular roadway section ($\theta_d > 0$). Considering the LEDs and PD located on the fronts and rears of the cars, respectively, and y measured with

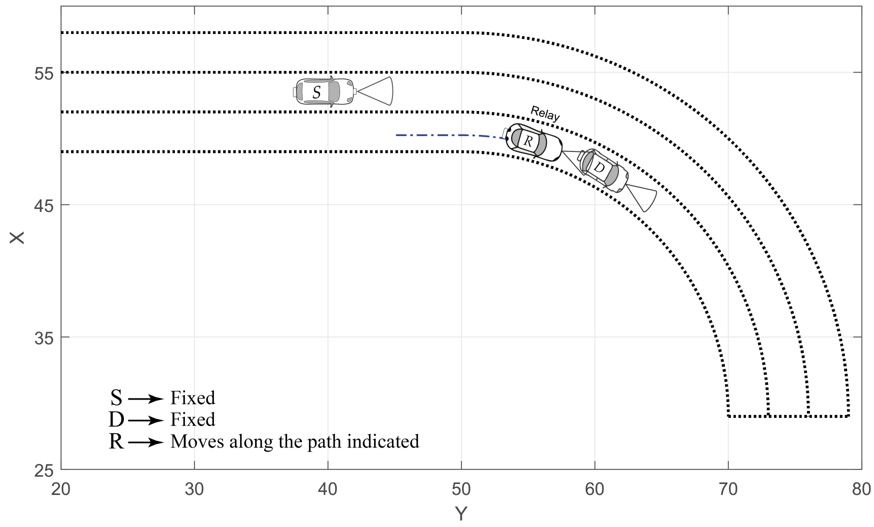

Figure 3.4: *Schematic of the cooperative communication along a curvilinear roadway. D is considered fixed at different angular positions, while R follows the dash-dotted path between S and D. For all cases S is considered as having $y_s < 50$ m.*

respect to the center of each car, we found

$$dsdy_{sd} = y_d - y_s - \frac{l_d}{2}\cos\theta_d - \frac{l_s}{2}, \tag{3.8}$$

$$dsdx_{sd} = x_d - x_s - \frac{l_d}{2}\sin\theta_d, \tag{3.9}$$

$$\phi_s = \arccos\left(\sin\gamma_s \cos\left[\alpha - \arctan\left(\frac{dsdx_{sd}}{dsdy_{sd}}\right)\right]\right), \tag{3.10}$$

$$\psi_d = \arccos\left(-\sin\gamma_d \cos\left[\beta - \arctan\left(\frac{dsdx_{sd}}{dsdy_{sd}}\right)\right]\right), \tag{3.11}$$

where $\beta = \pi - \theta_d$. To avoid using vehicle speeds, we analyze the V2V-VLC perfomance using a constant value for the difference $y_d - y_s = L$. This constraint is used to meet the limiting condition $\hat{n}_s \perp \hat{n}_d$; i.e., $\alpha = 0$ and $\beta = \pi/2$, when D reaches the end of the semicircular roadway in Figure 3.3. Thus, we found that the PD axis rotation can be easily written as $\theta_d = \tan^{-1}\left[\frac{y_s+L-h}{\sqrt{L^2-(y_s+L-h)^2}}\right]$ when moving along the curved road. These geometrical analyses are directly extended to the cooperative communication case by using the relays in the receiving and transmitting mode as the destination and source vehicle, respectively.

3.2 BER Analysis

In this section, we introduce the analysis of the cooperative FD V2V-VLC protocol. Self-interference is neglected for FD V2V-VLC, differently to the RF transmission, as the LED and PD are isolated. Hence, the received signal at node l of the signal from k can be expressed as:

$$v_{kl} \quad = \quad \zeta P_k H_{kl}(0) u_k + N_{kl}, \tag{3.12}$$

where P_k and u_k are the power and the message sent by the corresponding transmitter, respectively. N_{kl} represents the Gaussian additive noise at the node l, with variance σ^2, and ζ is the responsivity (at a fixed wavelength) of the photodiode expressed in A/W.

The signal to noise ratio (SNR) is calculated for the channel $k \to l$ as:

$$\text{SNR}_{kl} = \frac{[\zeta P_k H_{kl}(0)]^2}{\sigma^2}, \tag{3.13}$$

with $\sigma^2 = \sigma^2_{\text{shot}} + \sigma^2_{\text{thermal}}$ representing the noise variance; i.e., the sum of the shot noise and the thermal noise variances. The shot-noise variance is calculated by

$$\sigma^2_{\text{shot}} = 2q\zeta P_k H_{kl}(0) B + 2q\zeta P_{bg} I_2 B, \tag{3.14}$$

where q represents the electron charge, B is the considered bandwidth, P_{bg} is the background noise power and I_2 is the noise bandwidth factor of the background noise. The P_{bg} value used in this research work, was obtained from a Daylight Noise Model in [70] and which was used by other research works [88,90]. P_{bg} formula is time-variant and we have considered the maximum value ($16dBm$), in order to guarantee even a best-effort communication in a situation like at noon. W_{approx} is the analytical spectral irradiance, E_{det} is the irradiance that falls within the spectral range of the receiver. T_c is peak filter transmission coefficient, A is the photodetector incidence area and n denotes the internal refractive index of the optical concentrator.

$$E_{det} = \int_{\lambda_1}^{\lambda_2} W_{approx}(\lambda) d\lambda \tag{3.15}$$

$$P_{bg} = E_{det} T_c A n^2 \tag{3.16}$$

The thermal noise is generated within the transimpedance receiver circuitry [91] and its variance ($\sigma^2_{\text{thermal}}$) is expressed by:

$$\sigma^2_{\text{thermal}} = \left(\frac{8\pi K_b T_{\text{A}}}{G}\right) \eta A_{\text{p}} I_2 B^2 + \left(\frac{16\pi^2 K_b T_{\text{A}} \Gamma}{g_{\text{m}}}\right) \eta^2 A_{\text{p}} I_3 B^3, \tag{3.17}$$

where K_{b} is the Boltzman constant, T_{A} is the absolute temperature, G is the voltage gain in open loop, η is the capacitance per unit area of the photodetector, Γ is the noise factor of the FET (field-effect transistor) channel, g_{m} is the FET transconductance and I_3 is the noise bandwidth factor. The modulation used in this transmission is on-off-keying (OOK), as it is proposed in the IEEE 802.15.7 standard for VLC communication [1, 73]. The BER for each link is calculated as [92]

$$\text{BER}_{sr_r} = Q(\sqrt{\text{SNR}_{sr_r}}), \tag{3.18}$$

$$\text{BER}_{r_t d} = Q(\sqrt{\text{SNR}_{r_t d}}), \tag{3.19}$$

where the Q(·) function

$$Q(x) = \frac{1}{\sqrt{2\pi}} \int_x^{\infty} e^{\frac{-a^2}{2}} da, \tag{3.20}$$

represents the probability of a normal (Gaussian) random variable having a value grater than x standard deviations.

The overall error performance of the dual-hop cooperative communication scheme, considering the intermediary node r, is then given by

$$\text{BER}_{\text{coop}} = 1 - (1 - \text{BER}_{sr_r})(1 - \text{BER}_{r_t d}). \tag{3.21}$$

When direct transmission is possible, e.g., there is a LOS between S and D cars, the overall error performance of the non-cooperative scheme can be written as

$$\text{BER}_{sd} = Q(\sqrt{\text{SNR}_{sd}}). \tag{3.22}$$

3.3 Numerical Results and Discussions

This section presents a numerical study of the performance for the proposed V2V-VLC cooperative communication scheme. We used the parameters in Table 3.1 for all the simulations in this work, according to [38, 39]. The S vehicle was also considered to be transmitting beacons of length of 300 bytes (N $= 2400$ bits) [93] to obtain the numerical results.

Parameter	**Symbol**	**Value**
FOV of the receiver	ψ_c	$\pi/6$ rad
Half value angle of an LED	$\phi_{1/2}$	$\pi/12$ rad
Internal refractive index	n	1.5

Area of incidence at receiver	A_p	1 cm^2
Filter Transmission Coefficient	T_c	1
Detector Responsivity	ζ	0.56 A/W
Ambient Temperature	T_A	300 K
Open loop channel gain	G	10
FET Transconductance	g_m	30 mS
Fixed PD Capacitance/area	η	112 pF/cm^2
Noise Bandwidth Factor	I_2, I_3	$0.562, 0.0868$
Background Noise Power	P_{bg}	16 dBm
LED Power	P_k	0.3 W
Horizontal Inclination angle	α	0 rad
Horizontal Inclination angle	β	π rad
Vertical Inclination angle	γ_1, γ_2	$\pi/2$ rad
Transmission Rate	$\mathcal{R}$	20 Mbps
Electronic Charge	q	1.6021×10^{-19} C
FET Channel noise factor	Γ	1.5
Boltzmann Constant	K_b	1.3806×10^{-23} J/K
System Bandwidth	B	20 MHz
Number of bits	N	2400 bits

Table 3.1: *System parameters.*

3.3.1 Straight Road Scenario

In order to study the cooperative BER for different straight roadway scenarios, we evaluate four scenarios labeled as Scenarios A, B, C and D in Figure 3.5. For comparative purposes, we considered the same center-to-center horizontal distance (45 m) between the source and destination vehicles in all the scenarios, whereas the relay moves in between S and D with a minimum horizontal separation of 2 m from each. All cars are considered following rectilinear trajectories. To the center-to-center distance ($45m$), must be diminished $2.5m$ from the front-side of source S and $2.5m$ from back-side of the relay R, since each vehicle has a fixed length of $5m$. The same must be considered for the $R - D$ communication. This operation is considered in our graphic results.

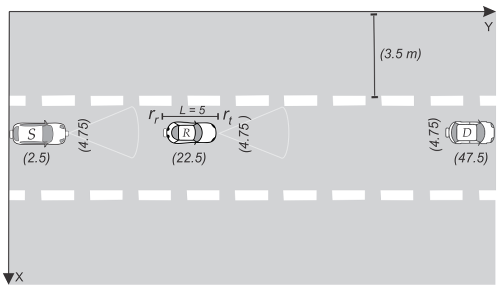

(a) *Scenario A.*

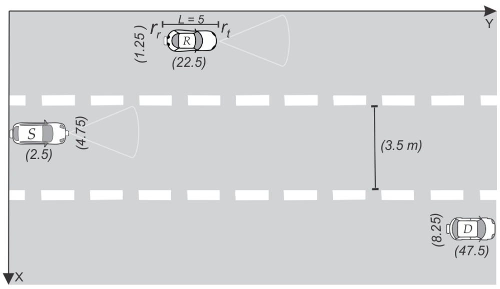

(b) *Scenario B.*

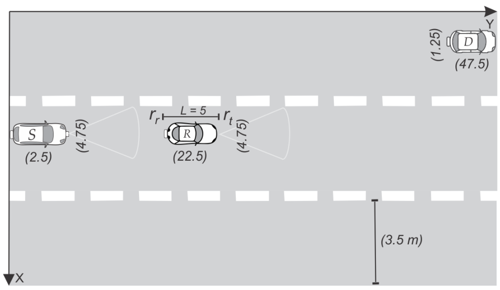

(c) *Scenario C.*

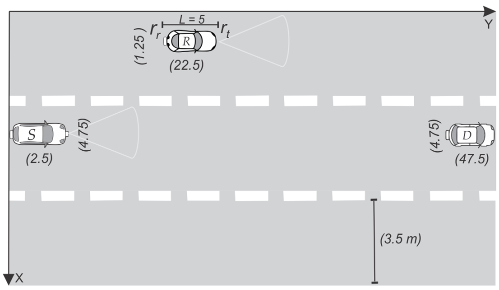

(d) *Scenario D.*

Figure 3.5: *Pictorial representation of the four different scenarios of simulation for the straight roadway case.*

Let us begin discussing the most simple case represented in Figure 3.5a; i.e., all cars are moving along the central lane. As the FOV is guaranteed for this rectilinear arrangement, this is also the best scenario. Numerical results for the cooperative BER for this case are presented by blue triangle-line in Figure 3.6.

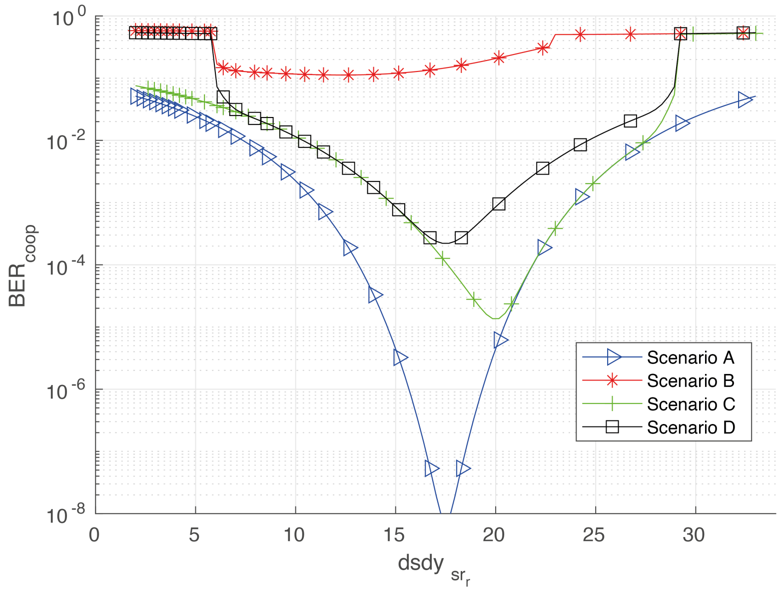

Figure 3.6: *Cooperative bit error rate (BER) for different scenarios. Calculations were made varying $dsdy_{sr_r}$ between S and D, which were considered 40 m apart from each other.*

An optimum cooperative BER is found for a source-relay distance of 17.5 m, which represents the case where the center of the relay is half the distance between S and D. From Figure 3.6, we also note that the cooperative BER tends to get worse for the scenarios B, C and D. In particular, the scenario B (Figure 3.5b) has the worst performance, as the relay is very far from the destination and cannot help the source in the absence of a LOS channel.

For a better explanation of the cooperative communication in this chapter, we extend the analysis of scenario D in Figure 3.7. From this last figure, it can be noted that the optimum value of the cooperative BER occurs when $\text{BER}_{sr_r} = \text{BER}_{r_t d}$, which represents the case where the center of the relay is half the distance between S and D. Such symmetrical behavior occurs because the source and destination are traveling along the same lane. As the relay R starts moving close to the source (S), this $S \Rightarrow R(r_r)$ communication is almost outside the FOV of $R(r_r)$, which explains the large BER values despite the small $dsdy_{s,r_r}$ distance. The same analysis applies for the symmetrical $R(r_t) \Rightarrow D$ communication link.

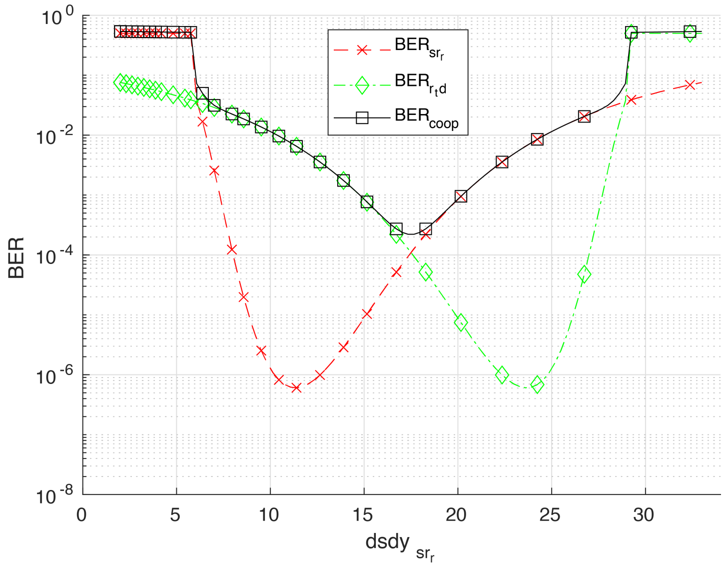

Figure 3.7: *Results for the cooperative BER associated with the scenario D in Figure 3.5d, considering an intermediate relay.*

3.3.2 Curved Road Scenario (Non-Cooperative Communication)

We will now discuss the BER for the vehicles communicating along the curved roadway scenario represented in Figure 3.3. As previously mentioned, the PD-axis rotates around the x-axis as D moves along the curved roadway section. In Figure 3.8a, we present the numerical results for the BER and the corresponding θ_d as function of y_s. We may note a constant BER $= 10^{-5}$ for $y_s \leq 30$ m, which corresponds to the straight roadway section $\theta_d = 0$. For $y_s > 30$ m, $0° < \theta_d \leq 90°$, we note an abrupt increase of the BER associated to a diminishing in the corresponding FOV at D. We can also note, from this figure, that there is a threshold $\theta_d = 16.8°$ ($y_s = 36.2$ m) above which the communication is disrupted; i.e., the BER becomes 0.5. The reason of a little downhill in 3.8a is due to source vehicle S and destination vehicle D are in parallel lanes, separated 20 m respect to y axis and moving along the path. Because of the described condition, the FOV of vehicle D is receiving light incidence in a minimal area until around 30 m, after this distance D starts to enter in the curved section, offering a more incidence area, as long as it turns. From the last, a big incidence area of light helps to diminish the BER, but unfortunately the D vehicle starts to lose LOS with the S vehicle, this is why the communication is completely lost and the BER reach its maximum value of 0.5. The corresponding channel disruption is presented in Figure 3.8b, where $H_{s,d}(0)$ is presented for V2V-VLC between S and D. Figure 3.8c presents the corresponding $dsdy_{s,d}$ and $dsdx_{s,d}$ distances as functions of y_s, from which we may only note a slight change, making evident that the communication disruption is completely due to the loss of FOV between S and D.

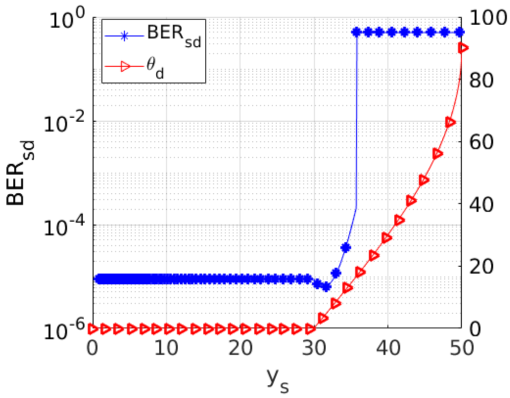

(a) *Numerical results for the BER and θ_d vs y_s, associated to the V2V-VLC between S and D.*

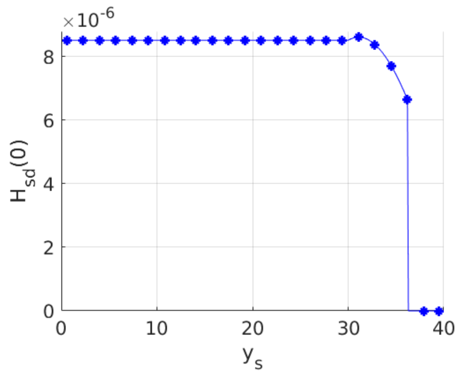

(b) *Numerical results for the LOS channel $H_{sd}(0)$.*

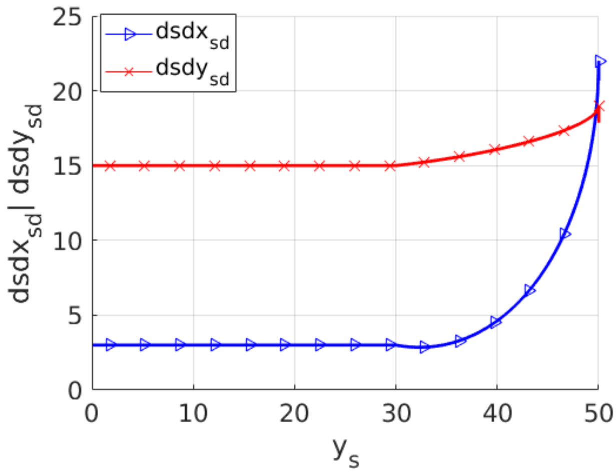

(c) *$dsdx_{sd}$ and $dsdy_{sd}$ as function of y_s.*

Figure 3.8: *Performance analysis of the non-cooperative V2V-VLC along a curved roadway scenario.*

3.3.3 Curved Roadway Scenario (Cooperative Communication)

In the previous subsection, for non-cooperative V2V-VLC, we found that the communication becomes disrupted for angles as small as $\theta_d > 16.8°$ ($\theta_s = 0°$). Here, we show that a cooperative V2V-VLC can be used to reach higher θ_d values. In doing so, we considered three cars named S, R and D moving along the roadway illustrated in Figure 3.4. As noted from the FOV analysis in Figure 3.6, the BER results exhibit acceptable values for cases where R and D, or S and R, travel along the same lane. In the curved scenario, the FOV changes dramatically in comparison to the rectilinear scenario. Thus, the analyses are limited to the scenario in Figure 3.4 in order to study the detrimental effects on the BER due to the curvilinear lanes. S and D were considered at different fixed positions while the relay vehicle R was moving along the entire path from S to reach D. For every D position exist a predefined S position, due to has been considered the $S - D$ path of the previous scenario in figure 3.3. In particular, results were calculated for D placed at $\theta_d = 25°, 30°, 35°$ and $40°$, as schematized in Figure 3.4. Results associated to the cooperative BER for these θ_d values are presented in Figure 3.9, from where we directly note that the communication link can be extended to angles up to $40°$ exhibiting good communication performances. The coordinates of the source and destination used for calculations in Figure 3.9, for different θ_d, are given by the Table 3.2. These results indicate that the cooperative V2V-VLC protocols constitute the most successful way to avoid communication disruptions for cars communicating along realistic curvilinear roadway scenarios. Furthermore, in the case of low-density-car highway environments, our results can be extended to properly use the highway VLC infrastructure in order to avoid communication disruptions.

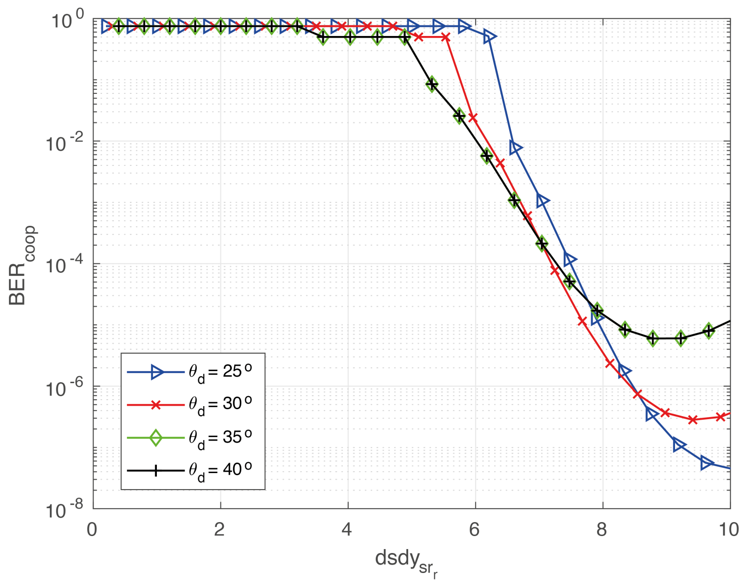

Figure 3.9: *Cooperative BER as a function of $dsdy_{sr_r}$ for different values of θ_d*

Table 3.2: *Coordinates of sources and destinations for different values of θ_d.*

Node Positions				
θ_d	x_s	y_s	x_d	y_d
25°	53.75 m	38.50 m	48.23 m	59.03 m
30°	53.75 m	40.00 m	47.40 m	60.62 m
35°	53.75 m	41.50 m	46.38 m	62.22 m
40°	53.75 m	42.90 m	45.24 m	63.71 m

In the next chapter, will be shown the analysis of the communication protocol in a scenario subject to interference of other vehicle.

Chapter 4

Analyses of Environmental Interference on V2V-VLC communication

In this chapter we analyzed a cooperative dual-hop visible light network operating with half-duplex and full-duplex protocols in a scenario subject to environmental interference of other vehicle.

4.1 System Model

We investigate an ad-hoc VLC vehicular network, referred to as V2V-VLC, see Fig 4.1, composed of a transmitting vehicle (S), a relay vehicle (R), a destination vehicle (D), and a potential interferer vehicle (I).

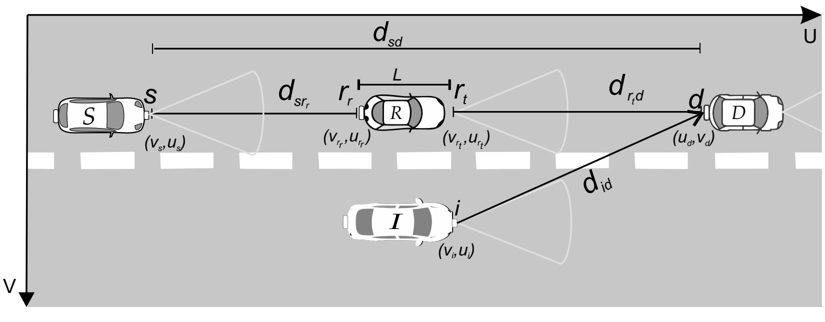

Figure 4.1: *V2V-VLC cooperative network with an relay and an interfering vehicle.*

The channel, $H_{k,l}(0)$, denoting the direct current gain, is one of the most important characteristics in VLC to estimate the achievable signal-to-noise ratio (SNR) for a fixed transmit power. Subindex $k \in \{s, r_t, i\}$ is used to denote each one of the possible transmitters in the system, while subindex $l \in \{r_r, d\}$ is used to represent the possible receivers (relay or destination vehicle). Before presenting an expression for $H_{k,l}(0)$, we need to perform a complementary geometrical analysis. In Figure 4.2 it is shown a pictorial representation of VLC-V2V mechanism for two vehicles along a road. Having into account that the lane runs along the u-axis, and its width along the v-axis, $\hat{n}_1$ and $\hat{n}_2$ are used to represent the transmitter and receiver axis, i.e., those are normal vectors to the LEDs surfaces, which are inclined by α (γ_1) and β (γ_2) respect to the v-axis (w-axis). ϕ_s and ψ_d are the irradiance and the incident angles respect to $\hat{n}_1$ and $\hat{n}_2$, respectively. Considering the distance between k and l along the u-axis (v-axis) as $\overline{u_{k,l}}$ ($\overline{v_{k,l}}$), and (v_k, u_k) $[(v_l, u_l)]$ as the coordinates of the transmitter (k) (receiver, l) in v-axis and u-axis, respectively. The angles ϕ_s and ψ_d are obtained as [43]

$$\phi_s = \arccos\left(\sin(\gamma_1)\cos\left[\alpha - \arctan\left(\frac{\overline{v_{k,l}}}{\overline{u_{k,l}}}\right)\right]\right), \tag{4.1}$$

$$\psi_d = \arccos\left(-\sin(\gamma_2)\cos\left[\beta - \arctan\left(\frac{\overline{v_{k,l}}}{\overline{u_{k,l}}}\right)\right]\right). \tag{4.2}$$

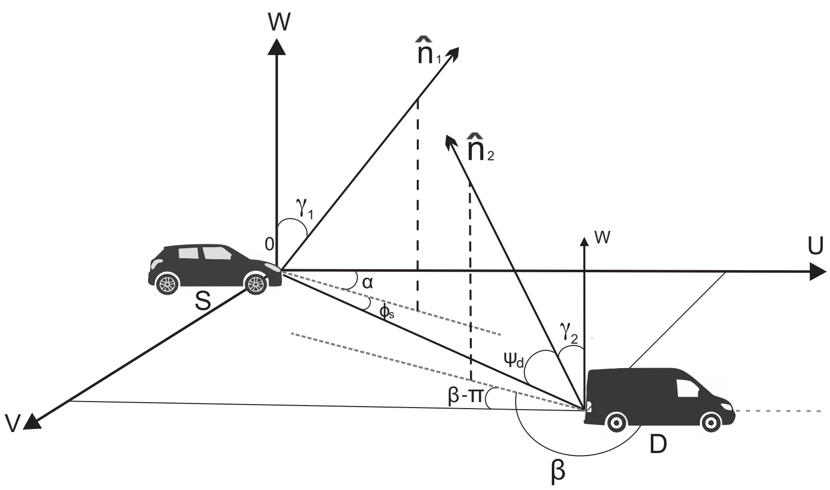

Figure 4.2: *Pictorial representation of two vehicles using VLC-V2V communication along a road. Parameters γ_1, γ_2, and ϕ_s depict the vertical inclination angles of the corresponding photoreceivers and the irradiance angle respect to $\hat{n}_1$. α and β are used to denote the horizontal inclination angles for $\hat{n}_1$ and $\hat{n}_2$, respectively. ψ_d denotes the incidence angle respect to $\hat{n}_2$, with $\hat{n}_1$ and $\hat{n}_2$ being the transmitter and receiver axis.*

Other important term for the calculation of $H_{k,l}(0)$ is the field of view (FOV) (limiting the gain), or aperture angle of the concentrator (ψ_c) (generally this is less than $\pi/2$), which depends on the refractive index (n) of the photodetector for computing the gain $g(\psi_d)$ and is modeled by [79]

$$g(\psi_d) = \begin{cases} \frac{n^2}{\sin^2(\psi_c)} & , 0 \leq \psi_d \leq \psi_c, \\ 0 & , \psi_d \geq \psi_c. \end{cases} \tag{4.3}$$

Since the LED surface is considered as an ideal Lambertian surface, the radiant intensity can be described by

$$\mathrm{R} = \left[\frac{(m+1)}{2\pi}\right] \cos^m(\phi_s). \tag{4.4}$$

The order-index, m, is given by $m = -\ln 2/\ln(\cos(\phi_{1/2}))$, where $\phi_{1/2}$ is a half value angle of an LED. Hence, $H_{k,l}(0)$ can be calculated as

$$H_{k,l}(0) = \left\{ \frac{\mathrm{R} A_\mathrm{p} T}{d_{k,l}^2} g(\psi_d) \cos(\psi_d) \quad , \quad 0 \leq \psi_d \leq \psi_c, \right. \tag{4.5}$$

where $d_{k,l}$ is the separation distance between the transmitter k and the receiver l, A_p is the area of incidence of the receiver (photodiode) and T_c is the filter transmission coefficient.

4.2 BER Analysis

In this section, we introduce the analysis of the cooperative schemes in a VLC network operating under the half-duplex and full-duplex protocols. For a full-duplex V2V-VLC network, the self-interference is neglected because the receiver and transmitter sensors are isolated. The received signals at the relay and at the destination can be expressed, respectively, as

$$y_{s,r_r} = \zeta P_s H_{s,r_r}(0) x_s + N_{s,r_r} + \zeta \delta_r P_i H_{i,r}(0), \tag{4.6}$$

$$y_{r_t,d} = \zeta P_{r_t} H_{r_t,d}(0) x_{r_t} + N_{r_t,d} + \zeta \delta_d P_i H_{i,d}(0), \tag{4.7}$$

where P_k and x_k are the power and the message sent by the transmitter k, respectively. $N_{k,l}$ represents the Gaussian additive noise at the node l, with variance σ^2, ζ is the responsivity of the photodiode, in A/W, for a certain wavelength (λ) and δ_l gives account of the interference by

$$\delta_l = \begin{cases} 1, & u_i < u_l, \\ 0, & \text{otherwise}, \end{cases} \tag{4.8}$$

where $\delta_l = 1$ represents the case in which the interferer vehicle causes interference to the receiver l.

The SINR is calculated for both channels, $s \to r$ and $r \to d$, by having into account the presence of an interferer vehicle as

$$\text{SINR}_{s,r_r} = \frac{[\zeta P_s H_{s,r_r}(0)]^2}{[\zeta \delta_r P_i H_{i,r_r}(0)]^2 + \sigma^2}, \tag{4.9}$$

$$\text{SINR}_{r_t,d} = \frac{[\zeta P_{r_t} H_{r_t,d}(0)]^2}{[\zeta \delta_d P_i H_{i,d}(0)]^2 + \sigma^2}, \tag{4.10}$$

where the noise variance σ^2 is the sum of the shot noise variance (σ^2_{shot}) shot and the thermal noise variance ($\sigma^2_{\text{thermal}}$). The shot noise variance is calculated by

$$\sigma^2_{\text{shot}} = 2q\zeta P_k H_{k,l}(0)B + 2q\zeta P_{bg} I_2 B, \tag{4.11}$$

where q represents the electron charge, B is the bandwidth considered, P_{bg} represents the background noise power and I_2 is noise bandwidth factor for the background noise. The thermal noise is generated within the transimpedance receiver circuitry [91] and its variance ($\sigma^2_{\text{thermal}}$) is expressed by:

$$\sigma^2_{\text{thermal}} = \left(\frac{8\pi K_b T_{\text{A}}}{G}\right) \eta A_{\text{p}} I_2 B^2 + \left(\frac{16\pi^2 K_b T_{\text{A}} \Gamma}{g_{\text{m}}}\right) \eta^2 A_{\text{p}} I_3 B^3, \tag{4.12}$$

where K_{b} is the Boltzman constant, in J/K, T_{A} is the absolute temperature, G is the voltage gain in open loop, η is the capacitance per unit area of the photodetector, Γ is the noise factor of the FET channel, I_3 is the noise bandwidth factor and g_{m} is the FET transconductance. For On-Off-Keying (OOK) modulation, the BER of each link can be calculated as [77]

$$\text{BER}_{s,r_r} = Q(\sqrt{\text{SINR}_{s,r}}), \tag{4.13}$$

$$\text{BER}_{r_t,d} = Q(\sqrt{\text{SINR}_{r,d}}), \tag{4.14}$$

where the Q(·) function represents the probability of a normal (Gaussian) random variable having a value grater than x standard deviations and is given by

$$Q(x) = \frac{1}{\sqrt{2\pi}} \int_x^\infty e^{\frac{-a^2}{2}} da. \tag{4.15}$$

When considering the intermediary node r, the overall error performance of the cooperative communication scheme is then given by

$$\text{BER}_{\text{coop}} = 1 - (1 - \text{BER}_{s,r_r})(1 - \text{BER}_{r_t,d}). \tag{4.16}$$

The corresponding throughput ($\mathcal{T}$) is limited by the cooperative BER (previously calculated) and the number of bits (N) used in the frame, for a given time slot, hence

$$\mathcal{T}_{\text{FD}} = \mathcal{R}(1 - \text{BER}_{\text{coop}})^{\text{N}}. \tag{4.17}$$

where $\mathcal{R}$ represents the transmission rate. The throughput $\mathcal{T}_{\text{FD}}$ is calculated with the product of the transmission rate $\mathcal{R}$ and the packet delivery rate (PDR),that is defined as the ratio of packets that are successfully delivered to a destination compared to the number of packets that have been sent out by the sender [94].

In the case of HD, the analysis is similar but as the transmission occurs within two time slots, the throughput of HD is reduced by a factor of $1/2$ in relation to the FD communication, i.e., $\mathcal{T}_{\text{HD}} = (1/2)\mathcal{T}_{\text{FD}}$.

4.3 Numerical Results and discussions

This section presents a numerical study of the performance of the proposed V2V-VLC cooperative communication schemes. The input parameters used in the calculations are presented in Table 3.3.1, in accordance to [38,43]. A relay vehicle is considered between the source and destination vehicles on a straight line. The vehicles move at constant speed and each vehicle has a length L of 5 meters. The source vehicle transmits beacons with length of 300 Bytes (N $= 2400$ bits) [93].

Fig. 4.4 shows the BER versus the distance between the source and destination (d_{sd}) for the cases with/without the presence of an interferer vehicle. Considering the source transmitter (s) as a reference at $(0, 0)$, the relay receiver (r_r) at $(0, \frac{d_{sd}-L}{2})$, the relay transmitter (r_t) at $(0, \frac{d_{sd}+L}{2})$ and the interferer transmitter (i) at $(3, \frac{d_{sd}-L}{2})$, as depicted in Fig. 4.3 for a particular case of $d_{sd} = 21$ meters.

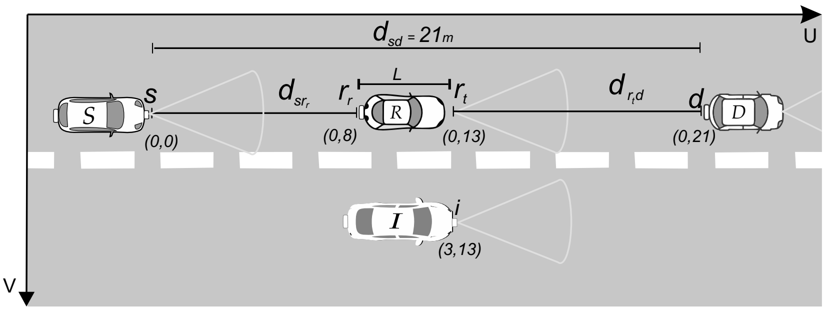

Figure 4.3: *Location of vehicles for the scenario of Figs. 4.4 and 4.5 .*

The Fig. 4.4 shows that the performance in terms of BER degrades with the presence of an interferer. For instance, the maximum d_{sd} in which BER $< 10^{-3}$ is 23 meters for the case with the presence of interferer, while the maximum d_{sd} is equal 51 meters for

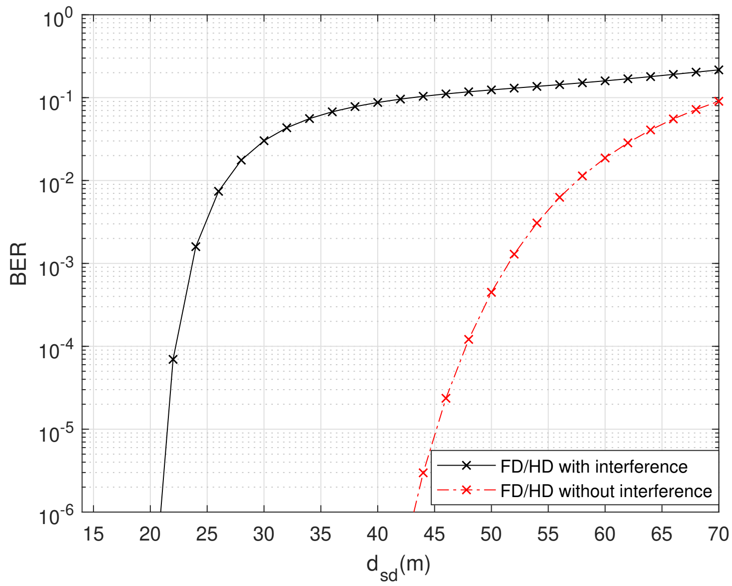

Figure 4.4: *BER as function of the distance source-destination for two different scenarios.*

the case without interference.

Fig. 4.5 shows the throughput versus the distance between the source and destination (d_{sd}) of HD/FD schemes for the cases with/without the presence of an interferer node. Note that the maximum throughput for $d_{sd} < 20$ meters for the scenario with

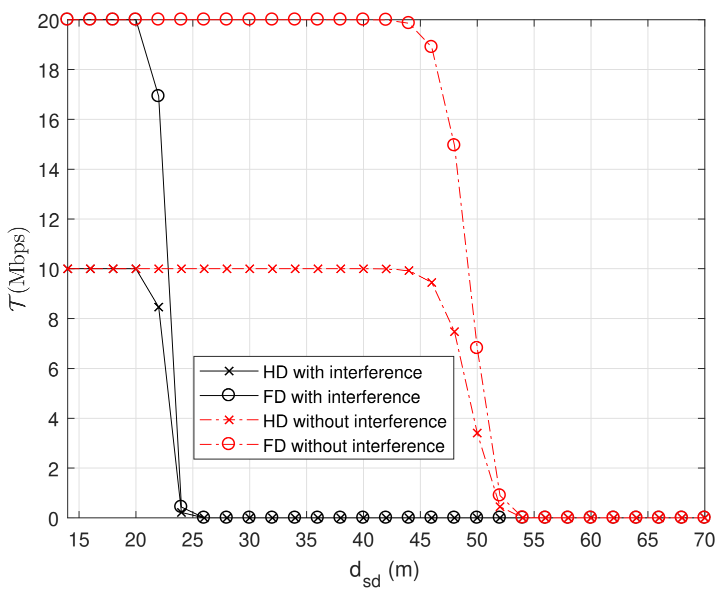

Figure 4.5: *Throughput as function of the distance source-destination of HD and FD schemes for two different scenarios.*

interference and $d_{sd} < 42$ meters for the interference free case.

Fig. 4.7 evaluates the BER versus the distance between the source transmitter and relay receiver (d_{sr_r}). Considering the the source transmitter (s) as a reference at $(0, 0)$, destination (d) is at $(0, 50)$, the transmitter (i) is positioned at three different locations in the lane next to the dual-hop network at $(3, 10)$, $(3, 23)$ and $(3, 40)$. The proposed configuration is depicted in the Fig. 4.6.

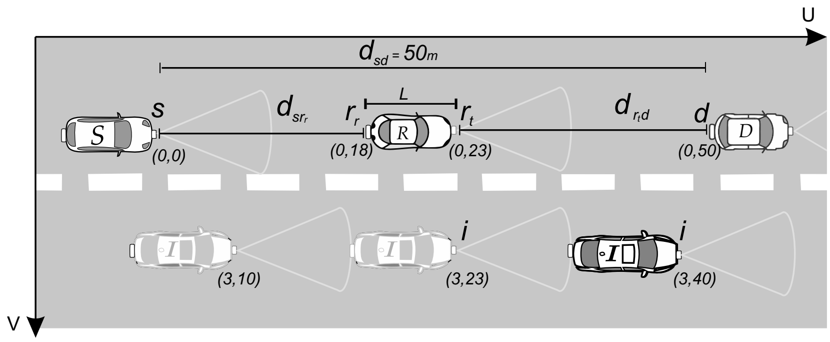

Figure 4.6: *Location of vehicles for the scenario of Fig. 4.7.*

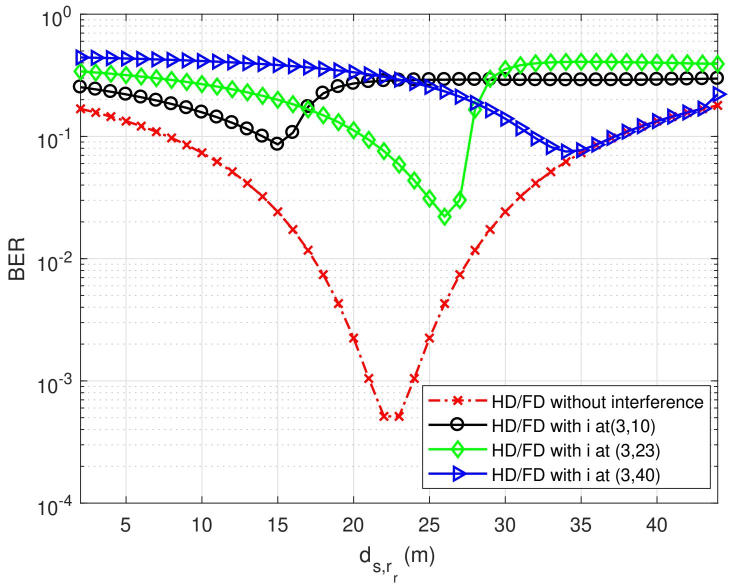

Figure 4.7: *BER as function of the distance source-relay for three different positions of the interferer vehicle.*

It is possible to see by the Fig. 4.7, that the best location for the relay vehicle is in the middle of the distance between source and destination for the scenario without interference. When the interferer is present the best location of relay is repositioned to next the source or destination in order to decrease the effect of interference. The optimal BER increases from $5{\cdot}10^{-4}$ to values in the order of 10^{-2}. Moreover, the scenarios with interference have little range with possible communication, for instance, when the interferer is located at $(3, 23)$, the communication can just occur for $20 < d_{sr_r} < 26$ meters, limiting the contribution of relay in the communication.

In the next chapter we will discuss our main results and come up with other open issues that might be addressed and developed in future works.

Chapter 5

Conclusions

Through this research, the effect of the application of VLC technology for network vehicular communications was studied in more detail. This contribution serves as the basis for those who are interested in pursuing this research line. After reviewing the literature on this topic, it was possible to verify that the approach of the previous authors did not include the study of a communication transition from a straight road to a curve, or jointly using cooperative communication through the use of intermediary vehicles. In addition, it was considered appropriate to study the effect of interferer vehicles, and how a relay vehicle can cooperate to transmit the message even with this external agent.

The study and knowledge acquired about VLC allowed us to develop the particular cases that arose as a proposal for this work. Just to comment on a few, there is a minimum range distance for destination vehicle can receive the information, these happens in the case where source and receiver are on parallel lanes and occurs due to the FOV angle of the photo-diode at the receiver vehicle. That is, the minimum separation distance that both vehicles must maintain is approximately 5.3 m under the conditions outlined in Chapter 4.

Another interesting result was the finding of the viability for establishing communication between source and destination vehicles along the road, even both being located on different lanes with a separation distance of up to 40m. This was possible using cooperative communication and all this only by applying VLC technology. Regarding the study of the communication transition from straight roads to curved roads, angle variations of up to 40 degrees were established for the communication link between the transmitter LED and the PD receiver, using cooperative communication too.

The performance of cooperative communications was evaluated through the rates obtained from BER. It was showed through different scenarios, which was the most optimal case for communication establishment. For example, look at the result presented in fig 4.2 where we analyzed four possible cooperative communication scenarios. The opportunities that were identified, little by little, were taking more concrete form, initially a general study was necessary, to know what could be a contribution based on what had already been done. Now, it can be said that everything that was planned at the beginning of this study was finally achieved. It was possible to design, schematize and carry out the geometric analysis.

After designing the code, it was possible to perform the corresponding simulations, which allowed discussing the results and contrasting them with with those in the literature. It was comforting knowing that the values obtained by simulation, in phases prior to the conclusion of this work, and that were related to experimental results of other authors, finally they were not very different. That is, it was possible to advance with much more confidence towards the final stages, knowing that the results of the simulation were close to the data obtained previously in an experimental way.

5.1 Future Works

After developing our research about cooperative full-duplex communication on straight and curved highways subject to interference, it could be interesting to specify other complementary research that adds value to the continuation of this work. The coexistence of a hybrid RF-VLC system could offer a greater range of communication to vehicles on the ad-hoc network. Another interesting improvement could be the evaluation of a vehicle to infrastructure (V2I) communication type and the study of randomness in the position of the transmitter vehicles in order to have a greater number of situations. Finally, the generation of a high density scenario of vehicles through simulation and experimental situations is a good challenge for future works.

References

[1] S. U. Rehman, S. Ullah, P. H. J. Chong, S. Yongchareon, and D. Komosny, "Visible light communication: A system perspective overview and challenges," *Sensors*, vol. 19, no. 5, 2019. [Online]. Available: http://www.mdpi.com/1424-8220/19/5/1153

[2] P. A. Haigh, F. Bausi, Z. Ghassemlooy, I. Papakonstantinou, H. L. Minh, C. Fléchon, and F. Cacialli, "Visible light communications: real time 10 mb/s link with a low bandwidth polymer light-emitting diode," *Opt. Express*, vol. 22, no. 3, pp. 2830–2838, Feb 2014.

[3] S. S. S. Yusof, N. M. Thamrin, M. K. Nordin, A. S. M. Yusoff, and N. J. Sidik, "Effect of artificial lighting on typhonium flagelliforme for indoor vertical farming," in *2016 IEEE International Conference on Automatic Control and Intelligent Systems (I2CACIS)*, Oct 2016, pp. 7–10.

[4] N. Yeh, T. J. Ding, and P. Yeh, "Light-emitting diodes light qualities and their corresponding scientific applications," *Renewable and Sustainable Energy Reviews*, vol. 51, pp. 55 – 61, 2015. [Online]. Available: http://www.sciencedirect.com/science/article/pii/S1364032115004505

[5] D. Barolet, "Light-emitting diodes (LEDs) in dermatology." *Seminars in cutaneous medicine and surgery*, no. 10.1016/j.sder.2008.08.003 [doi], dec 2008.

[6] K. D Desmet, D. Paz, J. J Corry, J. Eells, M. T.T. Wong-Riley, M. Henry Salzman, E. V Buchmann, M. P Connelly, J. V Dovi, H. L. Liang, D. Henshel, R. L Yeager, D. Millsap, J. Lim, L. Gould, R. Das, M. Jett, B. Hodgson, D. Margolis, and H. Whelan, "Clinical and experimental applications of NIR-LED photobiomodulation," *Photomedicine and laser surgery*, vol. 24, pp. 121–8, 05 2006.

[7] S. Yu, O. Shih, H. Tsai, N. Wisitpongphan, and R. D. Roberts, "Smart automotive lighting for vehicle safety," *IEEE Communications Magazine*, vol. 51, no. 12, pp. 50–59, December 2013.

[8] Y. H. Kim, W. A. Cahyadi, and Y. H. Chung, "Experimental demonstration of vlc-

based vehicle-to-vehicle communications under fog conditions," *IEEE Photonics Journal*, vol. 7, no. 6, pp. 1–9, Dec 2015.

[9] A. Bazzi, B. M. Masini, A. Zanella, and A. Calisti, "Visible light communications as a complementary technology for the internet of vehicles," *Computer Communications*, vol. 93, pp. 39 – 51, 2016.

[10] H. Farahneh, F. Hussain, and X. Fernando, "Performance analysis of adaptive ofdm modulation scheme in vlc vehicular communication network in realistic noise environment," *EURASIP Journal on Wireless Communications and Networking*, vol. 2018, no. 1, p. 243, Oct 2018.

[11] C. J. Rapson, B. Seet, P. H. J. Chong, and R. Klette, "Safety assessment of radio frequency and visible light communication for vehicular networks," *IEEE Wireless Communications*, pp. 2–8, 2019.

[12] A. Cailean and M. Dimian, "Current challenges for visible light communications usage in vehicle applications: A survey," *IEEE Communications Surveys Tutorials*, vol. 19, no. 4, pp. 2681–2703, Fourthquarter 2017.

[13] S. Rajagopal, R. D. Roberts, and S. Lim, "IEEE 802.15.7 visible light communication: modulation schemes and dimming support," *IEEE Communications Magazine*, vol. 50, no. 3, pp. 72–82, March 2012.

[14] T. D. C. Little, A. Agarwal, J. Chau, M. Figueroa, A. Ganick, J. Lobo, T. Rich, and P. Schimitsch, "Directional communication system for short-range vehicular communications," in *2010 IEEE Vehicular Networking Conference*, Dec 2010, pp. 231–238.

[15] L. Cheng, W. Viriyasitavat, M. Boban, and H. Tsai, "Comparison of radio frequency and visible light propagation channels for vehicular communications," *IEEE Access*, vol. 6, pp. 2634–2644, 2018.

[16] M. Falcitelli and P. Pagano, *Visible Light Communication for Cooperative ITS*. Cham: Springer International Publishing, 2016, pp. 19–47.

[17] I. Takai, T. Harada, M. Andoh, K. Yasutomi, K. Kagawa, and S. Kawahito, "Optical vehicle-to-vehicle communication system using LED transmitter and camera receiver," *IEEE Photonics Journal*, vol. 6, no. 5, pp. 1–14, Oct 2014.

[18] T. Komine and M. Nakagawa, "Fundamental analysis for visible-light communication system using LED lights," *IEEE Transactions on Consumer Electronics*, vol. 50, no. 1, pp. 100–107, Feb 2004.

[19] Y. Wang, , and and, "1.8-Gb/s wdm visible light communication over 50-meter outdoor free space transmission employing cap modulation and receiver diversity

technology," in *2015 Optical Fiber Communications Conference and Exhibition (OFC)*, March 2015, pp. 1–3.

[20] S. Wu, H. Wang, and C. Youn, "Visible light communications for 5G wireless networking systems: from fixed to mobile communications," *IEEE Network*, vol. 28, no. 6, pp. 41–45, Nov 2014.

[21] C. Wang, F. Haider, X. Gao, X. You, Y. Yang, D. Yuan, H. M. Aggoune, H. Haas, S. Fletcher, and E. Hepsaydir, "Cellular architecture and key technologies for 5g wireless communication networks," *IEEE Communications Magazine*, vol. 52, no. 2, pp. 122–130, February 2014.

[22] M. B. Rahaim and T. D. C. Little, "Toward practical integration of dual-use VLC within 5G networks," *IEEE Wireless Communications*, vol. 22, no. 4, pp. 97–103, August 2015.

[23] M. Ayyash, H. Elgala, A. Khreishah, V. Jungnickel, T. Little, S. Shao, M. Rahaim, D. Schulz, J. Hilt, and R. Freund, "Coexistence of WiFi and LiFi toward 5G: concepts, opportunities, and challenges," *IEEE Communications Magazine*, vol. 54, no. 2, pp. 64–71, February 2016.

[24] X. Li, R. Zhang, and L. Hanzo, "Cooperative load balancing in hybrid visible light communications and WiFi," *IEEE Transactions on Communications*, vol. 63, no. 4, pp. 1319–1329, April 2015.

[25] A. Nosratinia, T. E. Hunter, and A. Hedayat, "Cooperative communication in wireless networks," *IEEE Communications Magazine*, vol. 42, no. 10, pp. 74–80, Oct 2004.

[26] B. M. Masini, A. Bazzi, and A. Zanella, "Vehicular visible light networks with full duplex communications," in *2017 5th IEEE International Conference on Models and Technologies for Intelligent Transportation Systems (MT-ITS)*, June 2017, pp. 98–103.

[27] W. Shen and H. Tsai, "Testing vehicle-to-vehicle visible light communications in real-world driving scenarios," in *2017 IEEE Vehicular Networking Conference (VNC)*, Nov 2017, pp. 187–194.

[28] A. Memedi, H. Tsai, and F. Dressler, "Impact of realistic light radiation pattern on vehicular visible light communication," in *GLOBECOM 2017 - 2017 IEEE Global Communications Conference*, Dec 2017, pp. 1–6.

[29] L. U. Khan, "Visible light communication: Applications, architecture, standardization and research challenges," *Digital Communications and Networks*, vol. 3, no. 2, pp. 78 – 88, 2017.

[30] A. Ndjiongue and H. Ferreira, "An overview of outdoor visible light communications," *Transactions on Emerging Telecommunications Technologies*, vol. 29, no. 7, p. e3448, 2018.

[31] C. B. Liu, B. Sadeghi, and E. W. Knightly, "Enabling vehicular visible light communication (v2lc) networks," in *Proceedings of the Eighth ACM International Workshop on Vehicular Inter-Networking*, ser. VANET '11. New York, NY, USA: Association for Computing Machinery, 2011, p. 41–50.

[32] B. Tomaš, H. Tsai, and M. Boban, "Simulating vehicular visible light communication: Physical radio and mac modeling," in *2014 IEEE Vehicular Networking Conference (VNC)*, Dec 2014, pp. 222–225.

[33] A. Căilean and M. Dimian, "Current challenges for visible light communications usage in vehicle applications: A survey," *IEEE Communications Surveys Tutorials*, vol. 19, no. 4, pp. 2681–2703, Fourthquarter 2017.

[34] M. S. Islim, S. Videv, M. Safari, E. Xie, J. J. D. McKendry, E. Gu, M. D. Dawson, and H. Haas, "The impact of solar irradiance on visible light communications," *Journal of Lightwave Technology*, vol. 36, no. 12, pp. 2376–2386, June 2018.

[35] D. Cuba-Zúñiga, S. Mafra, J. Mejía-Salazar, S. Montejo-Sánchez, E. Fernandez, and S. Céspedes, "Visible light v2v cooperative communication under environmental interference," *XXXVII Brazilian Symposium on Telecommunications and Signal Processing SBrT 2019*, 2018.

[36] P. Luo, Z. Ghassemlooy, H. Le Minh, E. Bentley, A. Burton, and X. Tang, "Fundamental analysis of a car to car visible light communication system," in *2014 9th International Symposium on Communication Systems, Networks Digital Sign (CSNDSP)*, July 2014, pp. 1011–1016.

[37] Y. Al-Mayouf, M. Ismail, N. Abdullah, S. Al-Qaraawi, and O. Mahdi, "Survey on VANET technologies and simulation models," *ARPN Journal of Engineering and Applied Sciences*, vol. 11, no. 15, pp. 9414–9427, 2016.

[38] P. Luo, Z. Ghassemlooy, H. L. Minh, E. Bentley, A. Burton, and X. Tang, "Performance analysis of a car-to-car visible light communication system," *Appl. Opt.*, vol. 54, no. 7, pp. 1696–1706, Mar 2015.

[39] Z. Cui, P. Yue, and Y. Ji, "Study of cooperative diversity scheme based on visible light communication in vanets," in *2016 International Conference on Computer, Information and Telecommunication Systems (CITS)*, 2016, pp. 1–5.

[40] Gnawali, S. Yin, N. Smaoui, M. Heydariaan, and Omprakash, "Purple vlc: Accelerating visible light communication in room-area through pru offloading," in

Proceedings of the 2018 International Conference on Embedded Wireless Systems and Networks, ser. EWSN '18. USA: Junction Publishing, 2018, p. 67–78.

[41] P. H. Pathak, X. Feng, P. Hu, and P. Mohapatra, "Visible light communication, networking, and sensing: A survey, potential and challenges," *IEEE Communications Surveys & Tutorials*, vol. 17, no. 4, pp. 2047–2077, 2015.

[42] B. Soner and S. Coleri, "Visible light communication based vehicle localization and pose estimation," 2020.

[43] Z. Cui, P. Yue, and Y. Ji, "Study of cooperative diversity scheme based on visible light communication in vanets," in *2016 International Conference on Computer, Information and Telecommunication Systems (CITS)*, July 2016, pp. 1–5.

[44] B. M. Masini, A. Bazzi, and A. Zanella, "Vehicular visible light networks for urban mobile crowd sensing," *Sensors*, vol. 18, no. 4, p. 1177, 2018. [Online]. Available: https://www.mdpi.com/1424-8220/18/4/1177

[45] M. Y. Abualhoul, M. Marouf, O. Shagdar, and F. Nashashibi, "Platooning control using visible light communications: A feasibility study," in *16th International IEEE Conference on Intelligent Transportation Systems (ITSC 2013)*, Oct 2013, pp. 1535–1540.

[46] I. Takai, T. Harada, M. Andoh, K. Yasutomi, K. Kagawa, and S. Kawahito, "Optical vehicle-to-vehicle communication system using LED transmitter and camera receiver," *IEEE Photonics Journal*, vol. 6, no. 5, pp. 1–14, Oct 2014.

[47] A. T. Hussein, M. T. Alresheedi, and J. M. H. Elmirghani, "20 gb/s mobile indoor visible light communication system employing beam steering and computer generated holograms," *Journal of Lightwave Technology*, vol. 33, no. 24, pp. 5242–5260, 2015.

[48] H. Chun, S. Rajbhandari, G. Faulkner, D. Tsonev, E. Xie, J. J. D. McKendry, E. Gu, M. D. Dawson, D. C. O'Brien, and H. Haas, "Led based wavelength division multiplexed 10 gb/s visible light communications," *Journal of Lightwave Technology*, vol. 34, no. 13, pp. 3047–3052, 2016.

[49] T. Nawaz, M. Seminara, S. Caputo, L. Mucchi, F. S. Cataliotti, and J. Catani, "Ieee 802.15.7-compliant ultra-low latency relaying vlc system for safety-critical its," *IEEE Transactions on Vehicular Technology*, vol. 68, no. 12, pp. 12 040–12 051, Dec 2019.

[50] S. Arnon, "Optimised optical wireless car-to-traffic-light communication," *Transactions on Emerging Telecommunications Technologies*, vol. 25, no. 6, pp. 660–665, 2014. [Online]. Available: https://onlinelibrary.wiley.com/doi/abs/10.

1002/ett.2817

[51] M. Uysal, Z. Ghassemlooy, A. Bekkali, A. Kadri, and H. Menouar, "Visible light communication for vehicular networking: Performance study of a V2V system using a measured headlamp beam pattern model," *IEEE Vehicular Technology Magazine*, vol. 10, no. 4, pp. 45–53, Dec 2015.

[52] R. Mahendran, "Integrated lifi(light fidelity) for smart communication through illumination," in *2016 International Conference on Advanced Communication Control and Computing Technologies (ICACCCT)*, 2016, pp. 53–56.

[53] M. Leba, S. Riurean, and A. Lonica, "Lifi — the path to a new way of communication," in *2017 12th Iberian Conference on Information Systems and Technologies (CISTI)*, 2017, pp. 1–6.

[54] H. Haas, L. Yin, Y. Wang, and C. Chen, "What is lifi?" *Journal of Lightwave Technology*, vol. 34, no. 6, pp. 1533–1544, 2016.

[55] I. Yaqoob, I. A. T. Hashem, Y. Mehmood, A. Gani, S. Mokhtar, and S. Guizani, "Enabling communication technologies for smart cities," *IEEE Communications Magazine*, vol. 55, no. 1, pp. 112–120, 2017.

[56] S. Ayub, S. Kariyawasam, M. Honary, and B. Honary, "A practical approach of vlc architecture for smart city," in *2013 Loughborough Antennas Propagation Conference (LAPC)*, 2013, pp. 106–111.

[57] M. Figueiredo, L. N. Alves, and C. Ribeiro, "Lighting the wireless world: The promise and challenges of visible light communication," *IEEE Consumer Electronics Magazine*, vol. 6, no. 4, pp. 28–37, 2017.

[58] W. Ding, F. Yang, H. Yang, J. Wang, and X. Wan, "A hybrid power line and visible light communication system for indoor," *Computers in Industry*, vol. 68, pp. 170 – 178, 2015. [Online]. Available: http://www.sciencedirect.com/science/article/pii/S0166361515000160

[59] X.-W. Ng and W.-Y. Chung, "Vlc-based medical healthcare information system," *Biomedical Engineering: Applications, Basis and Communications*, vol. 24, no. 02, pp. 155–163, 2012. [Online]. Available: https://doi.org/10.4015/S1016237212500123

[60] A. E.-R. A. El-Fikky, M. E. Eldin, H. A. Fayed, A. A. E. Aziz, H. M. H. Shalaby, and M. H. Aly, "Nlos underwater vlc system performance: static and dynamic channel modeling," *Appl. Opt.*, vol. 58, no. 30, pp. 8272–8281, Oct 2019. [Online]. Available: http://ao.osa.org/abstract.cfm?URI=ao-58-30-8272

[61] F. Wang, Y. Liu, F. Jiang, and Nan Chi, "High speed underwater visible light

communication system based on led employing maximum ratio combination with multi-pin reception," *Optics Communications*, vol. 425, pp. 106 – 112, 2018. [Online]. Available: http://www.sciencedirect.com/science/article/pii/S0030401818303614

[62] G. Cossu, A. Sturniolo, A. Messa, S. Grechi, D. Scaradozzi, A. Caiti, and E. Ciaramella, "Sea-trial of an ethernet-based underwater vlc communication system," in *2018 Optical Fiber Communications Conference and Exposition (OFC)*, 2018, pp. 1–3.

[63] C. B. Liu, B. Sadeghi, and E. W. Knightly, "Enabling vehicular visible light communication (V2LC) networks," in *Vehicular Ad Hoc Networks*, 2011.

[64] M. Segata, R. Lo Cigno, H. M. Tsai, and F. Dressler, "On platooning control using IEEE 802.11p in conjunction with visible light communications," in *2016 12th Annual Conference on Wireless On-demand Network Systems and Services (WONS)*, Jan 2016, pp. 1–4.

[65] S. Yu, O. Shih, H. Tsai, N. Wisitpongphan, and R. D. Roberts, "Smart automotive lighting for vehicle safety," *IEEE Communications Magazine*, vol. 51, no. 12, pp. 50–59, December 2013.

[66] M. A. Vieira, M. Vieira, P. Louro, and P. Vieira, "Vehicular Visible Light Communication: a road-to-vehicle proof of concept," in *Optical Sensing and Detection V*, F. Berghmans and A. G. Mignani, Eds., vol. 10680, International Society for Optics and Photonics. SPIE, 2018, pp. 95 – 104.

[67] Y. Qiu, H.-H. Chen, and W.-X. Meng, "Channel modeling for visible light communications—a survey," *Wireless Communications and Mobile Computing*, vol. 16, no. 14, pp. 2016–2034, 2016. [Online]. Available: https://onlinelibrary.wiley.com/doi/abs/10.1002/wcm.2665

[68] Y. Akashi, J. Van Derlofske, J. Watkinson, and C. Fay, "Assessment of headlamp glare and potential countermeasures: Survey of advanced front lighting system (afs) research and technology," National Highway Traffic Safety Administration NHTSA, Tech. Rep. December, 2005.

[69] Z. Ghassemlooy, L. Alves, S. Zvanovec, and M. Khalighi, *Visible Light Communications: Theory and Applications*. CRC-Taylor & Francis Group, 2017.

[70] I. Lee, M. Sim, and F. Kung, "Performance enhancement of outdoor visible-light communication system using selective combining receiver," *IET Optoelectronics*, vol. 3, pp. 30–39(9), February 2009. [Online]. Available: https://digital-library.theiet.org/content/journals/10.1049/iet-opt_20070014

[71] C. G. Lee, "Visible light communication," in *Advanced Trends in Wireless Communications*, M. Khatib, Ed. Rijeka: IntechOpen, 2011, ch. 17. [Online]. Available: https://doi.org/10.5772/16034

[72] N. Kumar, M. Figueiredo, L. N. Alves, and R. L. Aguiar, "VLC Modulation Schemes," Instituto de Telecomunicações Pólo de Aveiro, Tech. Rep., 2010.

[73] I. C. S. Approved, "Ieee standard for local and metropolitan area networks: Short-range wireless optical communication using visible light," *IEEE Computer Society*, pp. 1–309, 2011.

[74] A. A. Qasim, M. F. L. Abdullah, R. Talib, H. M. gheni, K. A. Omar, and A. M. Abdulrahman, "Visible light communication the next future generation system," in *2019 International Conference on Information Science and Communication Technology (ICISCT)*, 2019, pp. 1–7.

[75] A. Mirvakili and V. J. Koomson, "High efficiency led driver design for concurrent data transmission and pwm dimming control for indoor visible light communication," in *2012 IEEE Photonics Society Summer Topical Meeting Series*, 2012, pp. 132–133.

[76] A. Duque, "Bidirectional visible light communications for the internet of things," Thesis, Université de Lyon, 2019.

[77] Z. Ghassemlooy, L. N. Alves, S. Zvanovec, and M.-A. Khalighi, *Visible light communications: theory and applications*. CRC press, 2017.

[78] M. Uysal, Z. Ghassemlooy, A. Bekkali, A. Kadri, and H. Menouar, "Visible light communication for vehicular networking: Performance study of a v2v system using a measured headlamp beam pattern model," *IEEE Vehicular Technology Magazine*, vol. 10, no. 4, pp. 45–53, 2015.

[79] J. M. Kahn and J. R. Barry, "Wireless infrared communications," *Proceedings of the IEEE*, vol. 85, no. 2, pp. 265–298, Feb 1997.

[80] J. Classen, D. Steinmetzer, and M. Hollick, "Opportunities and pitfalls in securing visible light communication on the physical layer," in *Proceedings of the 3rd Workshop on Visible Light Communication Systems*, ser. VLCS '16. New York, NY, USA: Association for Computing Machinery, 2016, p. 19–24. [Online]. Available: https://doi.org/10.1145/2981548.2981551

[81] D. Kedar and S. Arnon, "Non-line-of-sight optical wireless sensor network operating in multiscattering channel," *Appl. Opt.*, vol. 45, no. 33, pp. 8454–8461, Nov 2006. [Online]. Available: http://ao.osa.org/abstract.cfm?URI=ao-45-33-8454

[82] Y. Tanaka, S. Haruyama, and M. Nakagawa, “Wireless optical transmissions with white colored led for wireless home links,” in *11th IEEE International Symposium on Personal Indoor and Mobile Radio Communications. PIMRC 2000. Proceedings (Cat. No.00TH8525)*, vol. 2, 2000, pp. 1325–1329 vol.2.

[83] M. V. Bhalerao and S. S. Sonavane, “Visible light communication: A smart way towards wireless communication,” in *2014 International Conference on Advances in Computing, Communications and Informatics (ICACCI)*, 2014, pp. 1370–1375.

[84] M. Y. Abualhoul, M. Marouf, O. Shag, and F. Nashashibi, “Enhancing the field of view limitation of visible light communication-based platoon,” in *2014 IEEE 6th International Symposium on Wireless Vehicular Communications (WiVeC 2014)*, Sep. 2014, pp. 1–5.

[85] H. Farahneh, S. M. Kamruzzaman, and X. Fernando, “Differential receiver as a denoising scheme to improve the performance of v2v-vlc systems,” in *2018 IEEE International Conference on Communications Workshops (ICC Workshops)*, May 2018, pp. 1–6.

[86] D. J. Cuba-Zúñiga, S. B. Mafra, and J. R. Mejía-Salazar, “Cooperative full-duplex v2v-vlc in rectilinear and curved roadway scenarios,” *Sensors*, vol. 20, no. 13, p. 3734, Jul 2020. [Online]. Available: http://dx.doi.org/10.3390/s20133734

[87] W. Ciciora, W. Ciciora, D. Large, M. Adams, and J. Farmer, *Modern Cable Television Technology*, ser. Electronics & Electrical. Elsevier Science, 2004. [Online]. Available: https://books.google.com.br/books?id=tvUoQJXEwNEC

[88] Seok-Ju Lee and Sung-Yoon Jung, “A snr analysis of the visible light channel environment for visible light communication,” in *2012 18th Asia-Pacific Conference on Communications (APCC)*, 2012, pp. 709–712.

[89] C. Li, Y. Yi, K. Lee, and K. Lee, “Performance analysis of visible light communication using the stbc-ofdm technique for intelligent transportation systems,” *International Journal of Electronics*, vol. 101, no. 8, pp. 1117–1133, 2014. [Online]. Available: https://doi.org/10.1080/00207217.2013.809644

[90] P. Yue, L. Wu, and Z. Cui, “Integrating lte-d2d and vlc techniques to support v2v communication,” in *2017 IEEE/CIC International Conference on Communications in China (ICCC)*, 2017, pp. 1–6.

[91] H. Marshoud, P. C. Sofotasios, S. Muhaidat, G. K. Karagiannidis, and B. S. Sharif, “On the performance of visible light communication systems with non-orthogonal multiple access,” *IEEE Transactions on Wireless Communications*, vol. 16, no. 10, pp. 6350–6364, Oct 2017.

[92] Z. G. N. A. Zvánovec and M.-A. Khalighi, *Visible Light Communications Theory and Applications*. CRC Press Taylor & Francis Group, 2017, pp.273.

[93] M. Alam, J. Ferreira, and J. Fonseca, *Intelligent transportation systems: Dependable vehicular communications for improved road safety*. Springer, 2016, vol. 52.

[94] M. Jacobsson and C. Rohner, "Estimating packet delivery ratio for arbitrary packet sizes over wireless links," *IEEE Communications Letters*, vol. 19, no. 4, pp. 609–612, 2015.